

Progress and Perspective of Metal–Organic Frameworks as Solid Electrolyte Interphase Instability Mitigator in Magnesium Batteries

Manuel Salado,* Mega Kar, Senentxu Lanceros-Mendez, and Maria Forsyth

Understanding the stability and role of the solid electrolyte interphase (SEI) remains a challenge in lithium-ion batteries (LIBs). Factors such as electrolyte composition, temperature, charge-discharge rate, and state-of-charge strongly impact SEI stability and thickness. Magnesium batteries have gained attention due to their abundance, lower cost, better safety, and higher volumetric energy density than LIBs. However, their development is hindered by surface passivation of the Mg anode and sluggish ion transport due to an insulating SEI. Solid-state electrolytes (SSEs) offer improved stability, safety, and energy density over liquid

electrolytes. While the search for suitable SSE materials continues, recent advances—especially in metal-organic framework-based materials—show promise for enhancing magnesium battery performance. These advancements could expand their applications, from portable electronics to transportation. This study reviews the literature on magnesium batteries as an energy storage strategy. It highlights the importance of a bottom-up layer-by-layer approach and interface optimization to address challenges like low ionic conductivity and poor interfacial stability. Overcoming these barriers is essential for realizing the full potential of magnesium batteries.

1. Introduction

Promoting the use of electric vehicles (EVs) as well as achieving climate neutrality by 2050 are two of the initiatives included in the Green Deal with the aim to support the transition toward renewable energy, improving energy efficiency, reducing waste, and conserving biodiversity.^[1,2] In this regard, as the technology continues to evolve and the associated costs decrease, it is expected that EVs will become increasingly implemented in the coming years.

Lithium-ion batteries (LIBs) are currently the best candidates to support this mobility transition due to their high energy density (250–670 Wh L⁻¹), long cycle life (500–2000 charge cycles),^[3] low self-discharge, and a relative wide operating temperature range (−20–60 °C). In contrast, to cover the increasing performance requirements of LIBs for EVs, manufacturers are implementing new research aimed at improving safety, cycle stability, longevity, and reduce environmental impact of LIBs.^[4–7] This includes work on developing new materials for the battery electrodes (self-healing^[8] and self-sensing materials^[9]) and electrolytes (e.g., solid-state, phase-changing materials),^[7,10] as well as improvements in battery management systems and charging

infrastructure. Despite these efforts, there are still challenges related to scaling up LIBs, including limited lithium resources, concerns about the environmental impact of lithium mining, and competition from other energy storage technologies. Some examples of post-lithium-ion current technologies include solid-state batteries, sodium-ion batteries, zinc-air batteries, and metal-air batteries.^[11] However, these technologies are still in their early stages of development and commercialization, and it may take several years for them to become widely available and cost-effective.

In this scope, divalent ions such as calcium and magnesium (Ca²⁺ and Mg²⁺) have attracted increasing interest by their high theoretical volumetric capacity (2073 and 3833 mAh mL⁻¹, respectively) that in the case of Mg nearly doubles the volumetric capacity of lithium (2062 mAh mL⁻¹). Unfortunately, the current achievable capacity of this system in real conditions is in the order of 10–15% of the theoretical value.^[12,13]

Although magnesium-ion batteries offer several advantages over their lithium-ion counterparts, such as higher energy density, improved safety, and reduced risk of thermal runaway, they also face technical hurdles, including low power density, short cycle life, and sluggish ion transport.^[14] Mg metal anodes can be directly combined with Mg-free cathodes (such as CO₂, O₂, and S) to fabricate high-energy-density Mg metal batteries.^[15] While the feasibility of this concept has been demonstrated in principle, it has become apparent that conventional approaches to electrolytes and electrodes cannot be simply transferred or applied to magnesium battery technology, leading to more open questions than proper answers.

In this review, we briefly summarize the evolution of magnesium batteries materials as well as the main challenges they present to be a competitive technology for energy storage. In particular, we focus on recent advances devoted to develop novel solid electrolytes with the aim to avoid the surface passivation of Mg metal anode as well as to improve Mg-ion transport.

M. Salado, S. Lanceros-Mendez

BCMaterials

Basque Center for Materials

Applications and Nanostructures

UPV/EHU Science Park, 48940 Leioa, Spain

E-mail: manuel.salado@bcmaterials.net

M. Salado, S. Lanceros-Mendez, M. Forsyth

IKERBASQUE, Basque Foundation for Science

48009 Bilbao, Spain

M. Salado, M. Kar, M. Forsyth

Institute for Frontier Materials

Deakin University

Burwood, Victoria 3125, Australia

2. Rechargeable Mg Batteries: Their Evolution

In order for magnesium batteries to be competitive, the ideal cell design consists of a metallic magnesium anode and a cathode with a high reduction potential. With these premises, the selection of materials for the cathode is quite restricted.^[16,17] However, the biggest problem is the development of electrolytes that can withstand high potentials, since those used in lithium batteries (mostly carbonate-based) degrade at potentials above 3 V.

2.1. Cathodes

The development of cathodes in magnesium batteries is mainly focused on two types of materials: insertion materials with the aim of increasing the storage of magnesium ions in their structure^[18] and conversion materials to improve the kinetic processes at their interface.^[19] Aurbach et al.^[20] showed the feasibility of Chevrel phase molybdenum sulfide (Mo_6S_8) cathodes. Further studies^[21] demonstrated that the electron-deficient nature of Mo_6S_8 (S is at -2 oxidation state) compound has an important role in Mg insertion as the divalent Mg^{2+} ion insertion does not change the oxidation state of transition metal Mo.

In recent years, several advancements have been achieved in the development of suitable cathode materials for magnesium batteries. Various materials have been explored, including transition metal oxides,^[17] polyanions,^[22,23] and organic compounds,^[24] that can effectively intercalate magnesium ions. Some of the most promising cathode materials for magnesium batteries include magnesium titanium oxide,^[25] magnesium vanadium oxide,^[26] and magnesium iron phosphate.^[27] However, the diffusion of

divalent Mg ions in oxides is generally sluggish due to the strong electrostatic interactions with the oxygen lattice. To address this problem, there are two main possible ways: 1) increasing the operating temperature up to 150–300 °C to accelerate the diffusion of Mg^{2+} (that limits suitable applications); 2) finding a framework with lower activation energy for ion hopping (e.g., MOFs, functionalized materials).^[16,17,28,29] As one potential solution, the thiospinel Ti_2S_4 ^[30] showed low-volume expansion (<10%), good Mg^{2+} diffusivity ($5 \times 10^{-10} \text{ cm}^2 \text{ s}^{-1}$), and good cycling stability when it was tested at 60 °C. However, at room temperature (RT), plating/stripping reactions only occurred at very low c-rates (C/50). It was found that the preference of Mg^{2+} to occupy octahedral sites instead of tetrahedral could be the reason for a high-energy barrier. If we compare the Mg^{2+} intercalation process in a layered-sulfide cathode material, such as VS₄, Dey et al.^[31] reported three different mechanisms as depicted in Figure 1. First, an intercalation reaction (A to B), both intercalation and conversion reaction (B to D), and finally until further discharge at 0.3 V, conversion reaction is the dominant mechanism (D to E).

2.2. Anodes

Although Mg metal is the ideal candidate, a seminal work carried out by Zhang et al.^[32] unraveled the electrolyte chemical decomposition by introducing H_2O impurities into the conventional electrolyte. As conclusion, the main reason for electrolyte decomposition in electrochemical and/or chemical reaction pathways with inherent H_2O ligands is the formation of H_2O /diglyme solvating ion, such as $[\text{Mg}^{2+}(\text{H}_2\text{O})_6]^{2+}$. Consequently, current anodes remain inadequate to fully meet the demands of practical



Manuel Salado received his international and industrial Ph.D. in material science in 2017, from Abengoa Research along with Pablo de Olavide University. After his post-doctoral position as "Juan de la Cierva" (2018), currently, he is a Marie Curie Global Fellow (2022-2025) at Deakin University (Australia) and Basque Center for Materials, Applications and Nanostructures (Spain) to develop novel solid-electrolyte materials for energy storage. Specifically, his work is focused on the development of multifunctional materials to improve the electrolyte/electrodes interface. From 2024, he started the Ikerbasque research fellow position to continue his research at BCMaterials.



Mega Kar completed her doctor of philosophy (Ph.D.) at Monash University (2012-2015). She specializes in IL synthesis and electrochemistry, working on battery applications including lithium, sodium, and magnesium. In 2021, Dr Kar was also awarded the Alfred Deakin Research Fellow at Deakin University to develop novel low-cost and safe materials for zinc-air batteries. Currently, she is leading the research efforts in designing new salts, liquid, and solid-state materials for energy storage systems.



Senentxu Lanceros-Mendez is Ikerbasque professor at BCMaterials, Basque Center for Materials, Applications and Nanostructures, Leioa, Spain, where he is the scientific director. He is an associate professor at the Physics Department of the University of Minho, Portugal (on leave), which also belongs to the Center of Physics. He graduated in physics at the University of the Basque Country and obtained his Ph.D. degree at the Institute of Physics of the Julius-Maximilians-Universität Würzburg, Germany. His work is focused on the development of smart and multifunctional materials for sensors and actuators, energy, environmental, and biomedical applications.



Maria Forsyth is the director of ARC Industrial Transformation Training Centre for Future Energy Storage Technologies, former ARC Laureate fellow, and currently, an Alfred Deakin Professorial Fellow at Deakin University (DU) and an Ikerbasque visiting professor at University of the Basque Country. She is the deputy director of the Institute for Frontier Materials (IFM) at DU, where she leads the research effort in energy storage and corrosion science. She has worked at the forefront of energy materials research since her Fulbright Research Fellowship in 1990 and has consistently made breakthrough discoveries, including in polymer electrolytes, ionic liquids, and organic plastic crystals.

applications. A deeper understanding of the interfacial science and the morphological and compositional evolution of Mg metal anodes is crucial. A wide range of strategies have been developed to avoid the formation of the insulating solid electrolyte interphase (SEI). Among them, the use of functionalized MXene/graphene heterostructures,^[33,34] Mg alloys (e.g., Bi–Mg, Sn–Mg, Sn–Sb–Mg, Bi–Sn–Mg, or Ti–Mg),^[14] three-dimensional (3D) host nanostructure design, or surface modification has been successfully applied. Specifically, the use of a 3D hosts with a porous skeleton and high surface area can significantly reduce local current density and lower the Mg^{2+} nucleation threshold, thereby suppressing uneven magnesium stripping and plating (Figure 2a).^[35] Additionally, the robust structure and abundant porosity of these 3D hosts provide ample space to accommodate the electrode's volume changes during the Mg stripping/plating processes, which is advantageous for achieving stable and long-term cycling performance in rechargeable magnesium batteries (RMBs). Among the different promising material chemistry using this 3D design, carbonaceous hosts are the best candidates due to their large specific area, good electrical conductivity, large internal space, and high mechanical stability. For instance, Song et al.^[36] designed a vertically aligned nitrogen- and oxygen-doped carbon nanofiber arrays on carbon cloth (Figure 2b). They demonstrated as Mg electrodeposition follows a microchannel-filling growth mechanism, attributed to the host's uniformly arranged short nanoarray architecture, concave dimpled surface, and magnesiophilic properties. This design achieves a reduced nucleation overpotential of 647 mV and extends Mg plating/stripping cycle life to 110 cycles, even at a high current density of 10 mA cm^{-2} .

In addition to carbonaceous materials, MgO-coated Zn skeleton as the collector for anode-free Mg batteries by a facile control of the interfacial chemistry, was proposed.^[37] Inspired by this strategy, Mao et al.^[38] has recently suggested an anode-free $Mg_2Mo_6S_8$ -MgS/Cu batteries. In this system, $Mg_2Mo_6S_8$ catalyzes the decomposition of MgS (replenish fresh Mg for Mg loss caused by electrolyte corrosion) as well as provides strong adsorption to

the polysulfides (improving long-term cycling). As a result, a reversible capacity of 190 mAh g^{-1} with the capacity retention of 92% after 100 cycles was achieved (Figure 2c). Also, a promising energy density (420 Wh L^{-1}) was calculated promising the practicable application of Mg batteries.

Another strategy comprises the use of magnesium alloys, such as magnesium–lithium alloys, which can provide a higher electrode potential and better energy efficiency.^[39] Apart from Li, other elements have been recently tested with excellent results. After the inclusion of different elements (e.g., 1 at% Al, Zn, Mn, and Sn) in Mg alloys, Liu et al.^[40] demonstrated as only 1% Gd in the Mg alloy reduces the Mg^{2+} diffusion energy barrier of 0.34 eV improving the performance of a Gd// Mo_6S_8 cell battery with a capacity of 73.5 mAh g^{-1} at 5 C over 8000 cycles. Very recently, gallium metal was confined into graphene to add self-healing properties and consequently improve the stability of the anode in magnesium batteries. The strategy consisted in introducing a core–shell structure of Ga confined by reduced graphene oxide (Ga@rGO). As result, the cell retains the 66% of the specific capacity under an ultrahigh current of 1 A g^{-1} stable up to 700 cycles at a slightly elevated temperature of 40°C .^[41]

Besides the progress in electrolytes and cathode materials, various breakthroughs in the understanding, design, and fabrication of magnesium batteries have been achieved. For example, taking advantage of additive manufacturing, it is possible to develop 3D-printed magnesium batteries with higher energy density and faster charging times compared to traditional batteries.^[42,43] Moreover, the use of molecular dynamic simulations is paramount to understand both kinetic processes and local structures of different nanostructured materials and to properly understand the obtained experimental results to further tailor materials and structures toward high-performance batteries.^[32]

2.3. Organic Electrolytes

An ideal nonaqueous electrolyte should exhibit high ionic conductivity and effective transport of Mg^{2+} ions, along with

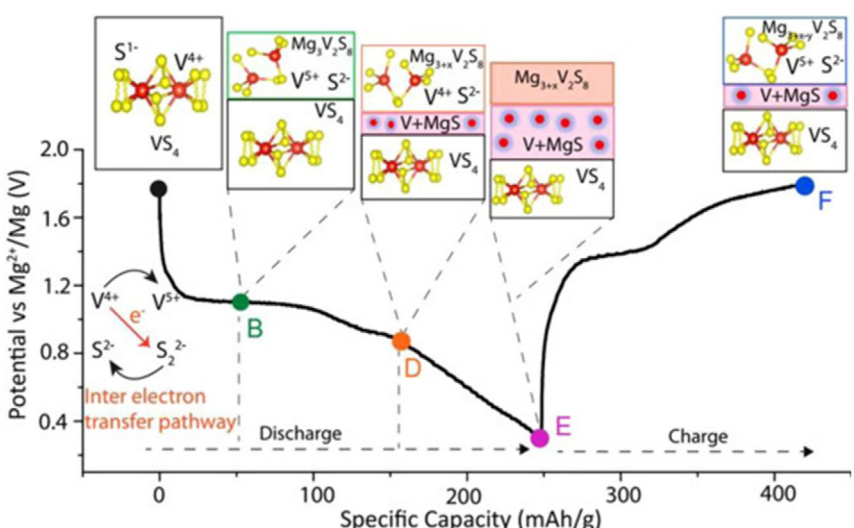


Figure 1. Schematic summarizing the redox processes occurred during de-magnesiation of VS_4 . The redox changes of V and S and the internal electron-transfer pathway during the initial magnesiation process. Reprinted with permission.^[31]

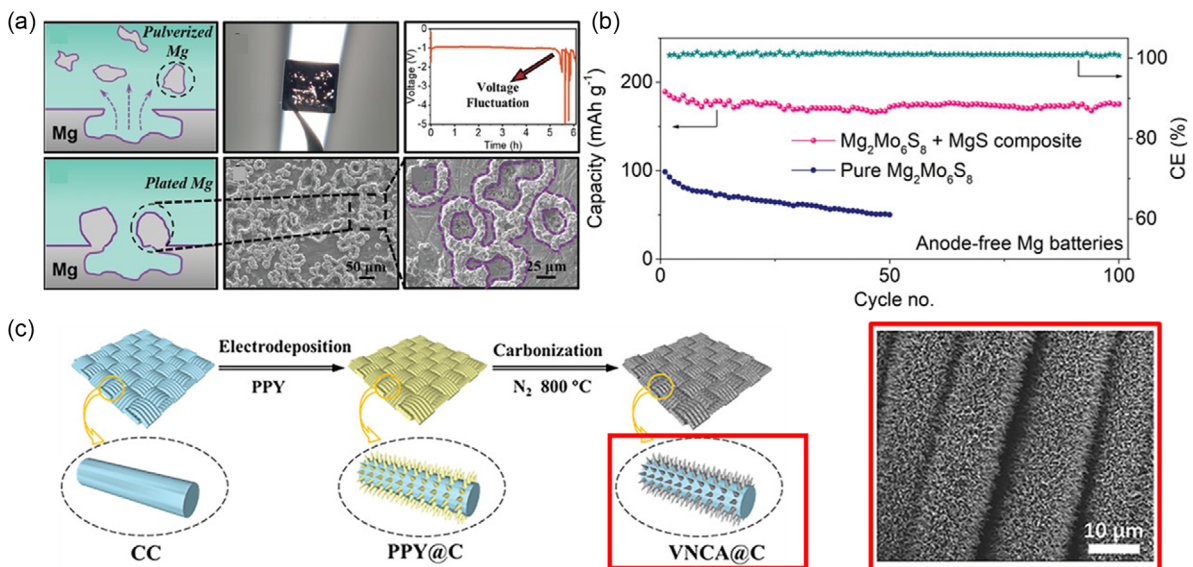


Figure 2. (First row from left to right) Schematic diagram of Mg-metal-anode fracture and pulverized Mg formed during the stripping process. a) Mg-metal electrode on the stripping side of an Mg//Mg symmetrical battery after stripping under 1 mA cm^{-2} and its galvanostatic polarization curve. (Second row from left to right) Schematic diagram of the plating morphology after stripping, and top-view scanning electron microscopy (SEM) images of the cycled Mg-metal anode, stripping under 1 mA cm^{-2} for 6 h. Reprinted with permission.^[35] b) Schematic illustration of the electrodeposition of 3D carbon skeleton (top-view SEM of VNCA@C). Reprinted with permission.^[36] c) Electrochemical performance of anode-free $\text{Mg}_2\text{Mo}_6\text{S}_8$ -MgS/Cu batteries. Long-term cycling stability for the first 100 cycles in MACC electrolyte at 20 mA g^{-1} . Reprinted with permission.^[38]

excellent electrochemical and chemical stability, low vapor pressure, and compatibility with magnesium. Achieving this compatibility has proven particularly challenging, as, unlike LIBs, the SEI layers formed at the Mg anode interface tend to be highly passivating. These layers are both ionically and electrically insulating, which impairs the transport properties of magnesium at the metal anode/electrolyte interface (see Figure 3a). Additionally, the use of organic solvents with high dielectric constants, such as carbonates and esters, leads to the formation of thick passivating layers that inhibit the electrochemical reversibility of Mg.^[44]

One of the earliest reports of the electrochemical reversibility of Mg was demonstrated by Liebenow et al.^[45] who focused on developing a family of electrolyte solutions based on highly reactive Grignard reagents (RMgX in ethereal solvents, where R = alkyl or aryl groups and X = halogen ligand, e.g., chloride). Soon after, Aurbach et al.^[46] expanded on the Grignard family to better elucidate their role in the Mg stripping/plating process and reported the weak interactions between Mg^{2+} ions and ethereal solvents that enhanced the electrochemical reversibility. Additionally, Grignard reagents in electrolytes can also help scavenge water and/or oxygen, inhibiting any decomposition reactions that may take place at the Mg anode. Nevertheless, to further enhance the ionic conductivity and anodic stability (1.5 V vs Mg/Mg²⁺), a large family of Grignard-based compounds was explored, many showing promising outcomes in the field of RMBs.

For example, the electrolyte comprised of $\text{Mg}(\text{AlCl}_2\text{BuEt})_2$ in tetrahydrofuran (THF) demonstrated electrochemical cycling of Mg (near 100% efficiency) as well as a discharge capacity of $>50 \text{ mAh g}^{-1}$ over 500 cycles in the presence of a Chevrel phase cathode.^[47]

More recently, uneven growth of Mg and Mg dendrites was observed in the presence of Grignard reagents under certain experimental conditions.^[48] Although numerous methods, such

as replacing alkyl R groups with phenyl moiety have been developed to improve these properties, the overall nucleophilic nature of Grignard reagent also remain a concern in RMBs. To overcome such challenges, nonnucleophilic compounds such as hexamethyldisilazane magnesium chloride (HMDSMgCl) and $\text{MgCl}_2\text{-AlCl}_3$ (MACC) in ethereal solvents were explored.^[49] The latter electrolyte, MACC, can generate the formation of chloride-containing dimer cations which weaken the interactions between Mg^{2+} ions, anions, and the solvent, enhancing the reduction stability of Mg. Despite these efforts, the use of chloride-based electrolytes still suffer from low anodic stability.^[15,50] Moreover, the electrochemical cycling of Mg from nonnucleophilic compounds such as HMDSMgCl can result in a porous morphology with an inhomogeneous SEI, reducing the lifetime drastically of RMBs.^[51]

To overcome these problems, research is currently focusing on “simple salt” electrolytes composed of solvated divalent Mg^{2+} cations ($\text{Mg}(\text{solvent})_n^{2+}$) which has been proven feasible for Mg deposition-stripping. Among them, $(\text{Mg}(\text{TFSI})_2)$, $(\text{Mg}(\text{BF}_4)_2)$, $\text{Mg}(\text{PF}_6)_2$, $\text{Mg}(\text{ClO}_4)_2$, and common aprotic solvents (DMSO, DMF, ACN). Nevertheless, the solvents, cation–anion interactions, and anionic stability have a strong influence on the SEI formation and thus on the electrochemical performance (Figure 3b).^[32,50,52] In the case of $\text{Mg}[\text{TFSI}]_2$, formation of ion-pairs and clusters is observed at the Mg anode/electrolyte interface upon electrochemical cycling of Mg. This is attributed to the strong coordination of Mg^{2+} ions with the anion, causing electrolyte degradation and poor electrochemical reversibility of Mg. Additionally, unlike monovalent cations, multivalent cations have higher charge densities (e.g., $\text{Li}^+ = 87$ vs $\text{Mg}^{2+} = 205$) leading to stronger interactions between metal cations and salt anions. For this reason, it is often challenging to obtain divalent salts without the presence of solvent molecules. For example, magnesium salts with $[\text{TFSI}]^-$

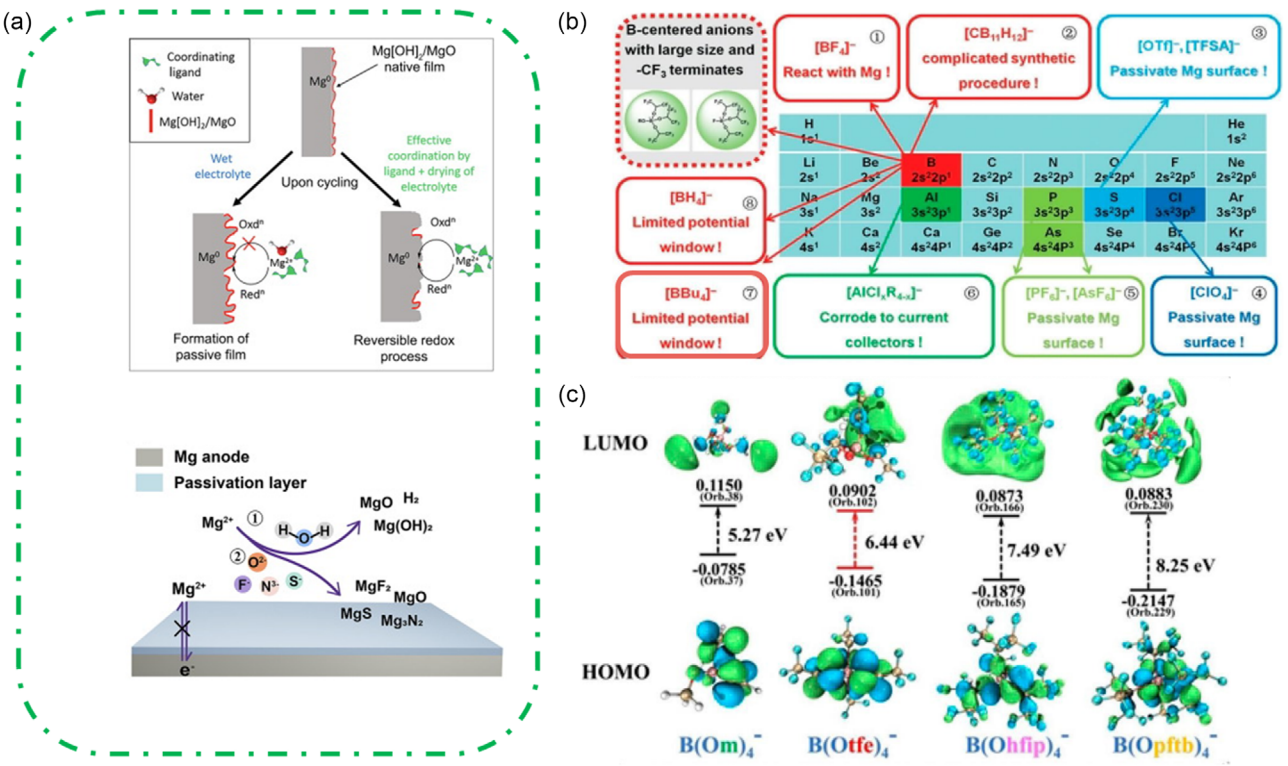


Figure 3. a) (Top) Scheme of the passivation film evolution when the electrolyte contains water and when an impurity-free electrolyte allows reversible deposition of Mg. (Bottom) Scheme of passivation layer formation mechanism and side-reaction products. Reprinted with permission.^[126] b) Chemical reactions of different elements from the periodic table. Reprinted with permission.^[127] c) Visualized LUMO/HOMO orbitals and transition gap energy of $\text{B}(\text{OR})_4^-$ anions. Reprinted with permission.^[54]

anions typically form in a hydrated state (e.g., $\text{Mg}(\text{H}_2\text{O})_6(\text{TFSI})_2 \cdot 2\text{H}_2\text{O}$) when recrystallized from an aqueous solution.^[53]

Therefore, the use of additives has been shown to alter the solvation of Mg^{2+} ions, promoting reversible Mg electrochemistry. For example, the addition of MgCl_2 and $\text{Mg}(\text{BH}_4)_2$ in low concentrations in $\text{Mg}(\text{TFSI})_2$ /glyme-based electrolytes is known to minimize the strong interactions between Mg^{2+} ions and $[\text{TFSI}]^-$ anions, facilitating Mg plating and stripping. The use of $[\text{BH}_4]^-$ has also been shown to successfully remove any water molecules from $\text{Mg}[\text{TFSI}]$ systems, that can often form $\text{Mg}(\text{OH})_2$ and MgO at the Mg anode-interface, inhibiting facile electrochemistry. However, even with the presence of such dehydrating agents and additives, high coulombic efficiencies (>99%) are often not achieved. Additionally, all of these systems suffer from low oxidation stability and Mg corrosion. More recently, the use of alternative weakly coordinating anions such as tetrakis, (hexafluoroisopropoxyloxy) aluminate ($[\text{Al}(\text{hfip})_4]^-$) or borates such as magnesium tetra(trifluoroethoxy)borate ($\text{Mg}[\text{B}(\text{OTFe})_4]$)^[54] and magnesium tetrakis(hexafluoroisopropoxy)borate ($\text{Mg}[\text{B}(\text{hfip})_4]$)^[33,55] have demonstrated facile Mg deposition–stripping with low overpotential, high oxidative stability, and high efficiency (Figure 3c). The presence of electron-withdrawing CF_3 groups in these anions makes it difficult to remove an electron at high-anodic potentials. Additionally, the high charge delocalization of the borate anions has been shown to enhance salt solubility, superior ionic conductivity, and high CE during electrochemical cycling of Mg. For example, the electrolyte comprised of 0.5 M $\text{Mg}[\text{B}(\text{hfip})_4]$ /DME demonstrated a high CE (98%) and low overpotential ($\approx 0.2 \text{ V}$).^[56]

Despite this, a nonuniform, porous SEI layer, comprised of C–F fragments and MgF_2 is formed upon cycling, indicating the instability of $[\text{B}(\text{hfip})_4]^-$ anion at the Mg anode interface. A more uniform and homogenous SEI was observed when the magnesium salt was replaced with the lithium analog, i.e., $\text{Li}[\text{B}(\text{hfip})_4]$ resulting in stable cycling of Mg in a $\text{Mg}-\text{Mo}_6\text{S}_8$ cell over 6000 cycles at 10C.^[57]

Another family of weakly coordinating borates is the closo-carborane i.e., $[\text{CB}_{11}\text{H}_{12}]^-$, which has also demonstrated high solubility and high ionic conductivity (0.85M $\text{Mg}[\text{CB}_{11}\text{H}_{12}]$ /glyme, 2.9 mS cm^{-1} at 25°C), owing to its nonnucleophilic nature and weak ion interactions. Interestingly enough, the anodic stability of closo-carborane anions is reported to be lower (4.6 V vs Mg/Mg^{2+}) than $[\text{TFSI}]^-$ and $[\text{BF}_4]^-$ anions in organic media. This is attributed to the oxidation of $[\text{CB}_{11}\text{H}_{12}]^-$ to the neutral radical $[\text{HC}\text{B}_{11}\text{H}_{12}]^-$. In contrast, the generation of this radical is not observed when the anion is present in its ionic liquid (IL) form,^[58] resulting in the anodic stability being as high as $[\text{TFSI}]^-$. Nonetheless, the synthetic route to carborane salts is toxic and costly. The lack of tailored ion-conducting surface films complicates the development of magnesium-anode batteries. A new approach, termed “artificial SEI” deposition, uses solvents, salts, and additives to create stable Mg ion-conducting films, enabling Mg anodes to function like lithium cells. Ban et al.^[59] reported a Mg^{2+} -conducting, electronic-insulating artificial interphase for Mg anodes, synthesized by mixing Mg powder, carbon black, polyacrylonitrile, and $\text{Mg}(\text{CF}_3\text{SO}_3)_2$, followed by thermal cyclization. The 100 nm thick interphase showed improved electrochemical performance, preventing passivation in vulnerable electrolytes.

2.4. Ionic-Liquid Electrolytes

Room temperature ionic liquids (RTILs) have garnered enormous attention in the battery field due to their advantageous properties as battery electrolytes. Particularly and in comparison, to organic electrolytes, RTILs have demonstrated low vapor pressure and low flammability as well as high thermal and electrochemical stability.

The first study exploring ILs as solvents for magnesium electrolytes investigated BmimBF_4 and $\text{Mg}[\text{TFSI}]_2$.^[60] Although reversible electrochemistry was reported and deposit products were obtained via galvanostatic deposition, the onset reduction potential was considerably more negative than -1.0 V versus Mg, and the cyclic voltammetric performance did not align with typical magnesium reduction and oxidation behavior. Subsequent studies using the same electrolytes demonstrated irreversible magnesium electrochemistry.^[61,62] Strong interactions between Mg^{2+} and $[\text{BF}_4]^-$ or $[\text{TFSI}]^-$ were thought to contribute to the high overpotential, which can lead to electrolyte decomposition and the formation of passivating precipitates on the electrode.

To date, electrochemical deposition of magnesium has been demonstrated in only a few RTILs.^[63,64] In 2016, Watkins et al.^[65] and Kar et al.^[66] simultaneously showcased the electrochemical reversibility of magnesium from magnesium borohydride in an IL composed of a polyether-based ammonium cation and bis(trifluorosulfonyl)imide anion. It was concluded that the ether group in these systems can substitute both $[\text{BH}_4]^-$ and $[\text{TFSI}]^-$ anions from the coordination sphere of Mg^{2+} , reducing the reductive decomposition of the TFSI anion and enhancing the transport of Mg^{2+} ions. To improve the oxidative stability of the electrolyte, Kar also reported using magnesium monocarbaborane ($\text{Mg}[\text{CB}_{11}\text{H}_{12}]_2$) in a similar IL.^[67] This highly inert and noncorrosive salt demonstrated excellent anodic stability ($>4.5\text{ V}$ vs. Li/Li^+). However, the poor solubility of the salt in the RTIL necessitated the addition of an organic solvent, ultimately achieving good compatibility with both magnesium and lithium.

RTILs utilized as cosolvents in magnesium electrolytes with THF or glymes significantly impacted electrochemical performance.^[68–70] Conductivity markedly increased after adding ILs; for example, conductivities of 0.33 and 7.44 mS cm^{-1} were recorded for EtMgBr/THF electrolytes before and after the addition of $\text{N,N-diethyl-N-(2-methoxyethyl)-N-methylammonium bis(trifluoromethanesulfonyl)imide}$ [DEME][TFSI].^[71] Notably, the conductivity of these mixed electrolytes surpassed that of the neat IL, attributed to enhanced ionic dissociation of magnesium salts in the mixed solvents, leading to an increase in charge carriers.

Thus, incorporating solvents into IL-based electrolytes enhances the mobility of Mg^{2+} ions, facilitates magnesium reduction and oxidation, reduces overall electrolyte costs, and maintains the high thermal and electrochemical stability characteristic of ILs.

2.5. Solid-State Electrolytes (SSEs)

To overcome the current challenges of liquid electrolytes, research in solid-state RMBs has garnered immense interest. However, the development of suitable SSEs for magnesium batteries has been challenging due to the difficulties associated with

producing practical Mg solid-electrolytes. For instance, inorganic ionic conductors such as spinel chalcogenides $[\text{MgX}_2\text{Z}_4]$, where X: In, Y, Sc, and Z: S or Se have demonstrated to be a fast Mg-ion solid conductor ($\sigma \approx 10^{-4}\text{ S cm}^{-1}$ for MgSc_2Se_4 at 25°C). However, its high electronic conductivity limits its application as a suitable solid ionic conductor. Phosphate- and boron-hydride-based materials have also been investigated for Mg-ion solid conductors. Between them, phosphate-based compounds deliver a very limited ionic conductivity ($\sigma \approx 10^{-6}\text{ S cm}^{-1}$ at 300°C), compared to $\text{Mg}(\text{BH}_4)_2$ -based materials which are very promising. Particularly, $\text{Mg}(\text{BH}_4)_2 \cdot 1.6\text{NH}_3$ delivered conductivities up to $\approx 10^{-5}\text{ S cm}^{-1}$ at RT and $\sigma \approx 10^{-3}\text{ S cm}^{-1}$ at 100°C . In addition, when metal oxide nanopowders (TiO_2) are combined with $\text{Mg}(\text{BH}_4)_2 \cdot 1.5\text{NH}_3$, $\sigma \approx 10^{-4}\text{ S cm}^{-1}$ at RT is achieved, demonstrating the effect of surface oxygen vacancy promotes the fast Mg^{2+} ion conduction.^[72] Nevertheless, further investigation should be addressed to improve their ionic conductivity as well as their stability and operational potential window (Figure 4a).^[15,73,74]

In this regard, novel strategies have been proved recently to improve ionic conductivity as well as better interface contact. The use of natural seed such as *Moringa oleifera* seed as membrane medium has been used after the inclusion of ZnO as semiconductor filler. The electrochemical properties indicated good ionic conductivities (e.g., 6.52 mS cm^{-1}) and an electrochemical stability of a $\text{Mg}/(\text{MoS}_2 + \text{graphite})$ full cell when the voltage is up to 2.34 V .^[75] Another strategy consists on the direct crystallization of a deep eutectic solvent. In particular, crystallizing $\text{Mg}(\text{TFSI})_2/\text{urea}$ improves the Mg^{2+} ion diffusion and augments the transference number.^[76] The role of the urea consists in dissociate Mg^{2+} and TFSI^- to form a $\text{Mg}^{2+}-\text{C=O}$ rich phase, with an optimum composition of $n_{\text{Mg}(\text{TFSI})_2}:n_{\text{urea}} = 1:8$ (molar ratio). When this material was tested in $\text{Mg}/\text{V}_2\text{O}_5$ full cells, delivered a high reversible capacity of 172 mAh g^{-1} as well as low overpotential when Mg stripping/plating was initially examined in symmetric cells (Figure 4b).

Early efforts to develop organic polymer electrolytes for magnesium batteries faced challenges in achieving high ionic conductivity, which is essential for efficient Mg^{2+} ion transport and battery performance.^[77] Initial approaches involved incorporating magnesium salts like MgCl_2 and $\text{Mg}(\text{ClO}_4)_2$ into a poly(ethylene oxide) (PEO) matrix.^[78] However, these attempts were hindered by poor Mg^{2+} migration, limiting conductivity and impeding progress. A breakthrough came in 1991 when Chen et al.^[79] synthesized a solid magnesium polyphosphonitrile sulfonate electrolyte with an ionic conductivity of $1 \times 10^{-8}\text{ S cm}^{-1}$, marking a significant step forward. In 1998, Liabenow^[80] synthesized a solid electrolyte using ethyl-magnesium bromide and PEO, achieving an improved ionic conductivity of $\approx 10^{-4}\text{ S cm}^{-1}$ at 50°C . These advancements spurred further development of organic polymer electrolytes for magnesium batteries. Nevertheless, previous studies concluded that Mg^{2+} is only mobile as long as the polymer is able to move with the ion (oligoether solvents), and ion motion was found to cease as the molecular weight increased. Recently, Nivetha et al.^[81] proposed polyvinyl butyral (PVB) doped with $\text{MgCl}_2 \cdot 6\text{H}_2\text{O}$ to improve thermal stability as well as better ionic conductivity ($1.9 \times 10^{-6}\text{ S cm}^{-1}$ at RT) and with an impressive transport number of 0.98.

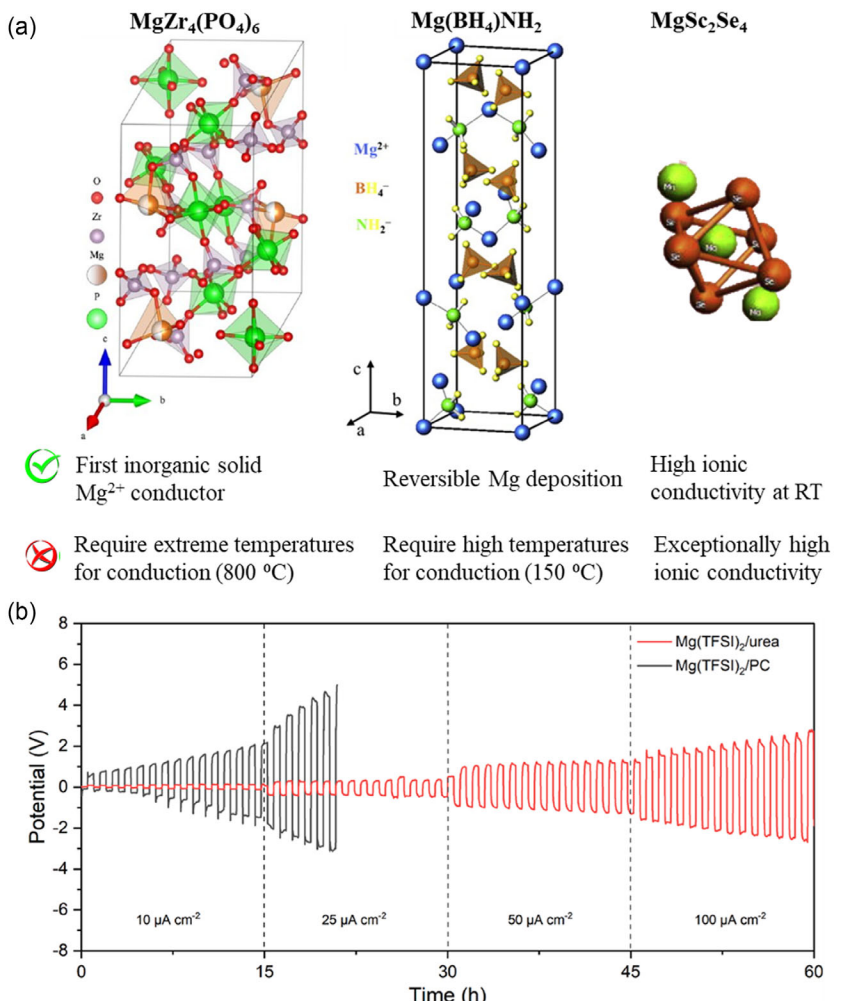


Figure 4. a) Scheme of the crystal structure of the most used inorganic solid electrolytes (the main properties are indicated). b) Voltage responses of Mg//Mg symmetric cells with MCE and Mg(TFSI)₂/PC electrolytes at current densities from 10 to 100 $\mu\text{A cm}^{-2}$. Reprinted with permission.^[76]

Contrary to inorganic conductors, improving ionic conductivity became a key focus in the search for better organic polymer electrolytes. One promising approach involved incorporating nanofillers into the polymer matrix. These nanofillers create additional pathways for ion transport and reduce the crystallinity of the polymer, which enhances ionic conductivity. For instance, Shao et al.^[82] synthesized Mg(BH₄)₂/PEO electrolytes with MgO nanoparticle fillers, achieving a high Coulombic efficiency of 98% during Mg electroplating/stripping. This demonstrated the potential of nanofiller-enhanced electrolytes in improving both battery performance and stability. Inspired by the success of quasi-solid LIBs,^[83] where the interface electrolyte/electrode is improved, an *in situ* crosslinked gel polymer electrolyte (e.g., magnesium tetrakis(hexafluoroisopropoxy)borate-based gel polymer electrolyte) was developed by Chen et al.^[84] With improved ionic conductivity (0.28 mS cm^{-1}), a overpotential below 0.1 V, and a Mg plating/stripping efficiency of 98.9% even after 1000 h of cycling. The Mo₆S₈//gel electrolyte//Mg pouch cells not only exhibited high energy density and excellent capacity retention but also demonstrated significantly enhanced safety, even after being physically cut. Moreover, it offers valuable insights

for the design and optimization of gel polymer electrolytes in advanced RMBs.

3. Challenges and Novel Strategies to Improve Interfacial Issues

Regardless of whether the focus relies on magnesium batteries or on other metals, the problem that comes with any multilayer technology based on interfaces with different materials is the understanding of surface/kinetic and/or degradation processes. Optimizing materials to avoid rapid degradation while achieving high efficiency is the greatest challenge. In the case of magnesium batteries, the situation is further complicated because the multielectron redox reaction leads to material restructuring in addition to a change in the oxidation state by 2 electrons.^[16]

Innovative approaches to enhancing the performance of Mg metal anodes primarily focus on interface engineering. A major challenge in utilizing Mg as an anode material is the formation of a passivation layer that impedes efficient Mg²⁺ ion transport, leading to poor battery performance. The strategies discussed

aim to address this by creating artificial interphases with tailored properties (**Table 1**). One significant method involves the chemisorption of sulfur dioxide (SO_2) gas onto the Mg surface.^[85] This process effectively transforms the native, insulating magnesium oxide (MgO) layer into a Mg^{2+} -conductive interphase, primarily composed of magnesium sulfite (MgSO_3). This modification drastically reduces charge transfer resistance, enabling reversible electrochemical reactions even in conventional ether-based electrolytes. Theoretical calculations density functional theory support that this interphase lowers the dissociation and migration energies of Mg^{2+} ions. The SO_2 treatment is also shown to be effective regardless of solvent or salt choice. Another approach utilizes phytic acid (PA) to create an artificial solid electrolyte interphase (SEI) layer on the Mg anode.^[86] The PA molecule coordinates with Mg^{2+} ions and forms a thin, porous film with 3D channels, facilitating uniform Mg^{2+} transfer and improving electrochemical performance. This porous structure allows for the formation of ion transfer channels crucial for Mg^{2+} transport. Additionally, the coordination with PA helps to reject most solvent molecules, preventing the formation of large electrolytic decomposition products. This leads to more uniform Mg deposition and improved cycling stability. The migration barrier of Mg^{2+} is lower when transferred through the coordination bonds along the PA skeleton.

A different strategy involves creating a multiphase artificial interphase through a substitution reaction between metallic Mg and a solution of antimony chloride (SbCl_3).^[87] This method results in an interphase primarily composed of metallic Sb,

intermetallic Mg_3Sb_2 , MgCl_2 , and SbCl_3 . The resulting interphase shows improved plating/stripping performance, with lower overpotentials and faster charge transfer kinetics. The Mg_3Sb_2 component has a lower Mg diffusion energy barrier, promoting swift Mg^{2+} migration. The insulating MgCl_2 layer also helps establish a potential gradient. A novel method involves the development of a glycerol α,α' -diallyl ether (GDAE)-based polymer electrolyte.^[88] This polymer is created through an anion modification strategy using magnesium salts containing polymerizable functional groups, coupled with a thiol-ene click chemistry polymerization approach. The resulting composite gel polymer electrolyte exhibits enhanced mechanical properties, high Mg^{2+} conductivity and transference number, and good compatibility with Mg anodes. This approach demonstrates the feasibility of anionic polymerization for RMBs. This polymer electrolyte demonstrates an "organic-inorganic hybrid" interface that provides long-term stability and cyclic durability. Researchers have also explored MOF membranes (more info in Section 4), specifically ZIF-8, grown directly onto Mg foil through electrochemical deposition.^[89] These membranes act as molecular sieves, allowing Mg ions to pass through while blocking larger solvent molecules like dimethoxyethane (DME). The self-correcting growth during the electrochemical deposition process ensures the formation of a defect-free membrane that prevents solvent permeation, inhibiting parasitic reactions. The incorporation of ILs into the MOF structure further enhances ionic conductivity. This approach effectively forms a stable and solvent-proof interphase, improving the electrochemical stability of the Mg anode. Table 1

Table 1. Comparison of different strategies and MOF interfacial mediators.

Interface approach	Battery types	Anode Cathode	Capacity retention/cycle	References
Structural and interface layers				
3D $\text{Fe}_3\text{O}_4/\text{C}$ composites	LIBs	$\text{Fe}_3\text{O}_4/\text{C} \text{Li}$	67%/1000	[128]
N_2 -doped carbon nanofiber-based 3D matrix	LIBs	$\text{NCNF} \text{LFP}$	82.4%/300	[129]
ALD Al_2O_3 -coated carbon shell	LIBs	ALD $\text{Al}_2\text{O}_3/\text{HCS} \text{Li}$	~500	[130]
polymer matrix (PA) and pore regulator (OV-POSS)	LMBs	$\text{Li} \text{Li}_4\text{Ti}_5\text{O}_{12}$	98%/300	[131]
Pyramid-type pattern	LIBs	$\text{Li} \text{LMO}$	88.7 %/450	[132]
Amorphous MgO -wrapped Zn-skeleton	RMBs	$\text{Mg}-\text{metal} \text{Mo}_6\text{S}_8$	98%/250	[37]
Mg^{2+} -conducting polymeric film (phytic acid (PA))	RMBs	$\text{PA}-\text{Al}@\text{Mg} \text{Mo}_6\text{S}_8$	99.8%/3000	[133]
MgF_2 -rich SEI	RMBs	$\text{Mg} \text{Mo}_6\text{S}_8$	99.5%/600	[88]
zeolite-polymer membranes	RMBs	$\text{Mg} \text{Mo}_3\text{S}_4$	91%/200	[134]
Gradient organic-inorganic SEI	RMBs	$\text{Mg} \text{Mo}_6\text{S}_8$	84%/200	[135]
3D magnesiphilic vertical carbon nanofiber arrays	RMBs	$\text{Mg} \text{o}_6\text{S}_8$	92%/700	[36]
MOFs				
ZIF-7	ZIBs	Zn/MnO_2	88.9%/600	[136]
Zn-MOF	LIBs	Li/Li	97.7%/250	[137]
UIO-66	ZIBs	Zn/MnO_2	~500	[138]
HKUST-1	ZIBs	Zn/MnO_2	97%/600	[139]
UIO-66	LIBs	Li/LiCoO_2	80%/250	[140]
MOF-808	LIBs	Li/LiFeO_4	93%/200	[141]
Mg-MOF layer	RMBs	$\text{CuS} \text{Mg}$	70%/40	[87]
MOF/Mg	RMBs	$\text{MOF}@\text{Mg} \text{V}_2\text{O}_5$	77%/30	[142]

provides an overview of several methods used to enhance the interaction between the anode and the electrolyte.

To get an idea of the challenges involved in developing RMBs, **Scheme 1** summarizes the materials used so far, showing that there is still important work to be done to achieve fully functional competitive batteries. However, although the development of divalent batteries entails the design of the different materials required as well as the control of the interfaces of the different battery components, previous knowledge is a great starting point.^[90]

4. The Role of MOFs as Interface Mediator

4.1. Approach 1. MOFs-Based Solid Electrolyte

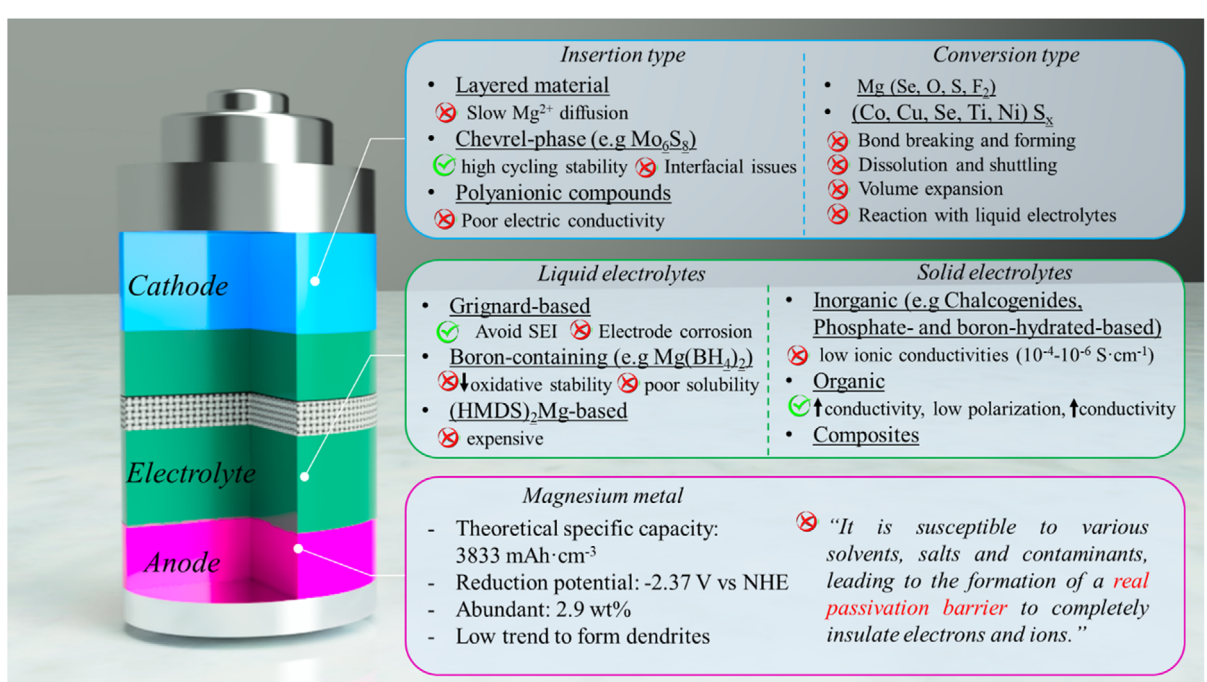
Although all components of the magnesium cell need to be developed to maximize battery performance, in this section, we will focus on the novel strategies for SSEs. The primary factor contributing to the limited conductivity of Mg^{2+} in solid-state materials is the strong electrostatic interaction with neighboring anions. This is largely due to the closely-packed crystal structures that are typically found in conventional solid-state materials, which can hinder the mobility of Mg^{2+} carriers. Therefore, it is envisaged that, if the crystal structure and surrounding environment are well-designed, a solid-state high-conductivity material is well within reach, which could revolutionize a range of industries such as electronics, energy storage, and transportation. For instance, the Mg^{2+} intercalation reaction reversibility of cathodes and anodes could be greatly improved by regulating the compatibility between the electrolyte and the nanostructured electrodes.

As we have aforementioned in the previous section, MOFs have been identified as potential materials for battery components

due to their crystalline and porous nature, high surface area, and structural tunability. It has been extensively demonstrated that MOFs can serve as electrodes in LIBs, as well as host materials, separators, or catalysts in metal–sulfur and metal–air batteries.^[91–93] In particular, the wide range of possibilities that MOFs offer, not only includes their use as a SSE, but also the possibility to modify the interfaces of the electrodes.^[94–96]

In this regard, Aubrey et al.^[97] were pioneers in the design of a Mg-based MOF as Mg^{2+} conductors ($Mg_2(dobpdc)$ ($dobpdc4^- = 4,4'-dioxidobiphenyl-3,3'-dicarboxylate$)) with ionic conductivities ($2.5 \times 10^{-4} S\text{ cm}^{-1}$) similar to spinel chalcogenides but at RT. Two of the key parameters regarding the tuneability of MOFs to enhance ionic diffusion are the pore size and the crystal structure. Nevertheless, the interactions within the framework and transport processes for these guest electrolytes might have a strong effect. Preferably, the anion should show little or no preference for absorption in the framework.^[98]

Although Mg-based MOFs would be desired for Mg batteries to avoid the presence of different metal ions, other metal-based MOFs have been used as ion conductors in RMBs. In 2017, Park et al.^[99] proposed a Cu(II)–azolate MOF ($(CH_3)_2NH_2[Cu_2Cl_3BTDD] \cdot (DMF)_4(H_2O)_{4.5}$ (MIT-20)) as a tuneable solid electrolyte. After soaking in $MgBr_2$, it exhibited a Mg ionic conductivity of $8.8 \times 10^{-7} S\text{ cm}^{-1}$ at RT. Two years later, $Cu_4(tppm)_2 \cdot 0.6CuCl_2$ (where tppm = tetrakis(4-tetrazolylphenyl)methane) improved in three order of magnitude ($1.3 \times 10^{-4} S\text{ cm}^{-1}$) the ionic conductivity of its previous counterpart (MIT-20).^[100] By tuning the channel configuration and introducing coordinatively unsaturated metal sites, it is possible to reach low activation energy (**Figure 5a**), which can be confirmed as a fast Mg-ion conductor. Very recently, Yoshida et al.^[101] reported a solid-state crystalline “ Mg^{2+} conductor” showing a superionic conductivity of around $10^{-3} S\text{ cm}^{-1}$ at ambient



Scheme 1. Summary of the main challenges in the different components for rechargeable Mg cells.

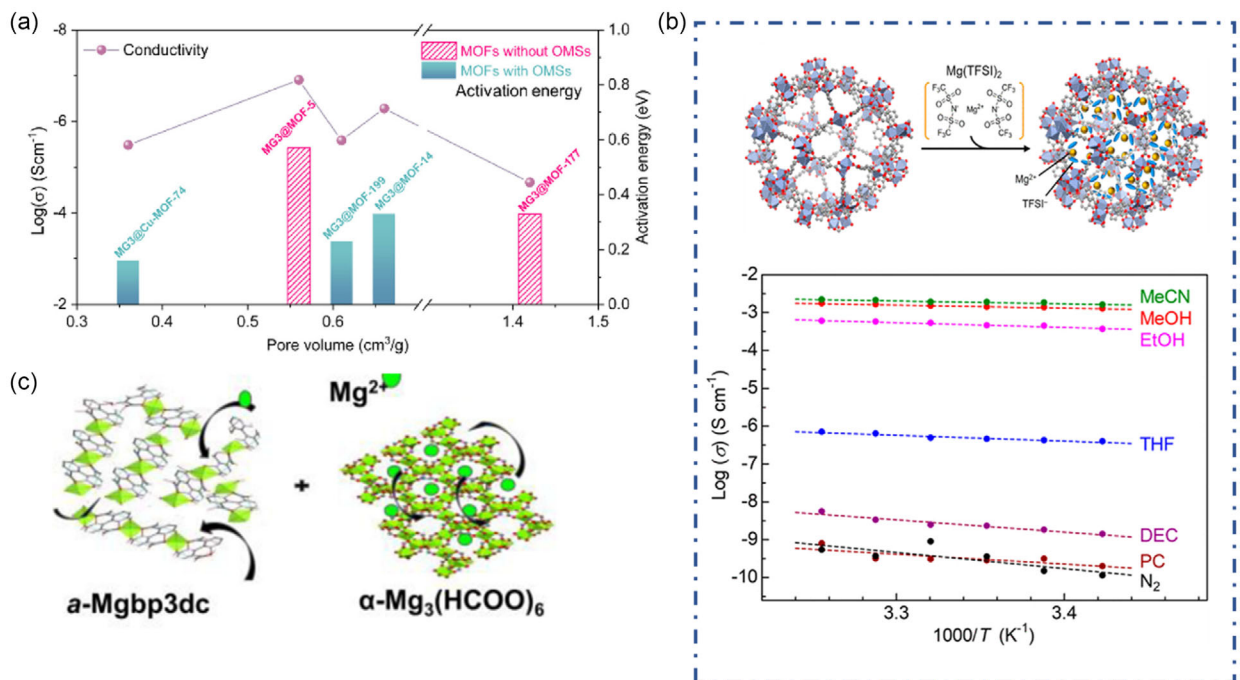


Figure 5. a) Comparison of the activation energies and conductivities of five MG3@MOFs electrolytes versus their pore sizes, indicating the effect of pore size and open-metal sites on Mg-ion conduction. Reprinted with permission.^[98] b) Schematic illustration of $\text{Mg}(\text{TFSI})_2$ inclusion inside the pores of MIL-101 (top) and temperature dependence of ionic conductivity of $\text{MIL-101}\supset\{\text{Mg}(\text{TFSI})_2\}_{1.6}$ under various guest vapors or dry N_2 . Reprinted with permission.^[101] c) Mg insertion mechanism of $\alpha\text{-Mgbp3dc}/\alpha\text{-Mg}_3(\text{HCOO})_6$ mixtures. Reprinted with permission.^[102]

temperature (Figure 5b), which was obtained using the large three-dimensional (3-D) pores (maximum ≈ 32 vs 21 \AA of Aubrey's work) of MIL-101, as ion-conducting pathways. This result demonstrated the importance to optimize the identity, geometry, and distribution of the cation hopping sites. Hassan et al.^[102] demonstrated as increasing the defective sites in MOFs are ways to enhance their performance as metal ion semi-solid electrolytes (Figure 5c). In particular, $\alpha\text{-Mgbp3dc}/\alpha\text{-Mg}_3(\text{HCOO})_6$ mixtures showed an order of magnitude improved ionic conductivity ($3.8 \times 10^{-5} \text{ S cm}^{-1}$) compared to single-phase $\alpha\text{-Mg}_3(\text{HCOO})_6$ as well as an activation energy for ion diffusion of only 0.22 eV.

To have a fully understanding and to upscale MOF-based batteries for a commercial use, research efforts need to be directed toward the development of highly conductive MOF composites or MOF-derived materials. It has been proven that pressed pellets often featured electrical resistance ($>5000\text{ }\Omega$) that is too high for practical applications. Furthermore, the existence of inevitable gaps between adjacent particles makes it exceedingly complex to unravel the true behavior of MOF as selective ionic conductors.^[103] Bearing this in mind, instead of pressed pellets, Luo et al.^[104] synthesized a Mg-MOF-74 thin film directly supported on anodized aluminum oxide (AAO) as Mg-ion conductor. Successful cycling of over 100 cycles was achieved with a low overpotential ($<0.3\text{ V}$) at a current density of 0.05 mA cm^{-2} . Control experiments demonstrated that Mg-MOF-74 thin films effectively blocked solvents (e.g., PC) and anions (e.g., TFSI^-) from crossing between the anolyte and catholyte. As a result, ionic conductivity of $3.17 \times 10^{-6} \text{ S cm}^{-1}$ at RT was achieved, showing similar values to previous reports Figure 6, where pressed pellets were used.^[97,99,100]

4.2. Approach 2. MOFs as Interlayers

In particular, the wide range of possibilities that MOFs offer, not only includes their use as a SSE, but also the possibility to modify the interfaces of the electrodes.^[94–96] In this regard, a permselective membrane of MOF ZIF-8, was synthesized directly on Mg surface.^[89] This angstrom scale membrane can precisely separate the solvent molecules from the MOF channels. As a result, a low-overpotential plating/stripping was achieved through the suppression of the permeation of solvents.

Development of novel hierarchical electrodes will entail greater specific capacity at low and high current densities, and greater cycling stability. In addition, that engineered surface will minimize concentration polarization losses, and enhance wettability within the electrolyte. The growth and specific characteristics of the MOF layer would be dependent on the method used to synthesize it. The multilayered approach was studied by Glaser et al.^[105] using MgSc_2Se_4 spinel as main conductor material and an electron-blocking $\text{UiO}66\text{-MgIL}$ interlayer reducing the Mg-ion migration barrier and therefore improving the electrolyte/electrode interface contact. Using MOF as a self-standing layer, Lee et al.^[106] synthesized Mg-MOF-74 films formed on silicon substrates for their possible use in anodes for magnesium batteries. It was demonstrated that the use of a mixture of acrylic acid and hydrofluoric acid facilitates the nucleation of MOF by the formation of carboxylic functional groups on the silicon surface. Another approach consists in taking advantage of the MOF microstructure as a scaffold to grow different materials.^[107] In this scope, Hu et al.^[108] synthesized NiSe_2 microspheres derived from Ni-MOFs and wrapped with reduced graphene oxide (NiSe_2/rGO),

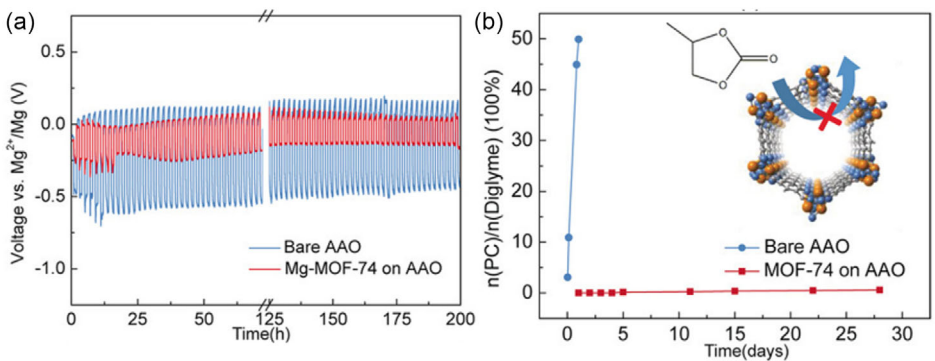


Figure 6. Properties of Mg-MOF-74 as a membrane in a practical electrochemical cell. a) Electrochemical features of Mg plating/stripping in an asymmetric cell at 0.05 mA cm^{-2} for 2 h each cycle. b) Negligible solvent (PC) crossover was measured when Mg-MOF-74 film was used as a separator (red); the crossover was significant when bare AAO was used (blue).

and used them as cathode material for RMBs. It was demonstrated that graphene improves the activity of the tiny NiSe₂ nanoparticles, enhancing the interphase charge transfer and the magnesium storage performance. As a result, the cells delivered a capacity of 215.5 mAh g^{-1} as well as good cycling stability over 300 cycles. Recently, a vertically oriented Mg/MOF layer was engineered by Wang et al.^[109] on the surface of Mg foil, serving as a Mg²⁺ reservoir and directing the controlled growth of Mg through a heteroepitaxial growth strategy (Figure 7a). Designed with abundant Mg²⁺ affinity sites and 1D-aligned MOF channels, the MgMOF layer facilitates rapid Mg²⁺ transport and homogeneous nucleation, reducing nucleation overpotential for the MgMOF@Mg anode. Additionally, the MgMOF layer acts as a protective barrier, preventing parasitic reactions and promoting uniform Mg electrodeposition. Electrochemical testing reveals

significant improvements with the MgMOF@Mg anode. The assembled symmetric cell exhibited an extended lifespan of 1200 cycles at a high current density of 8 mA cm^{-2} without short circuits. Furthermore, a full cell using a Mo₆S₈ cathode demonstrated outstanding cycling performance, maintaining 80.56% of its capacity after 14,000 cycles at 50°C (Figure 7b). This work offers new insights into the design of MOF-based protective layers, suggesting that a lattice geometrical perspective can be broadly applied to other advanced metal batteries. The enhanced performance is attributed to synergistic effects of precise lattice matching, a magnesiophilic interface, and an electrical-field effect.

Magnesiophilic scaffolds absorb Mg²⁺ better than Mg substrates due to abundant magnesiophilic sites, reducing short circuits from poor wettability and adhesion. Increasing the electrode's

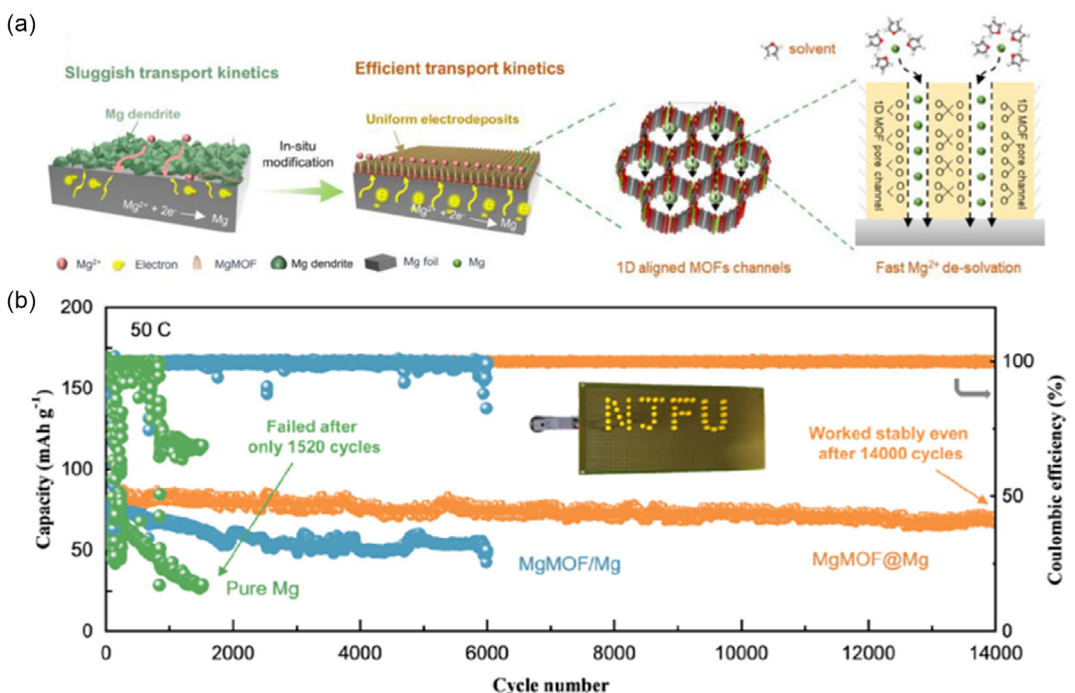


Figure 7. a) Structural organization and the proposed mechanism of interface kinetics of Mg electrodeposition for bare Mg and MgMOF@Mg anode. b) Cycling performance of the Mo₆S₈//Mg batteries assembled with bare Mg, MgMOF/Mg, and MgMOF@Mg anodes. Reprinted with permission.^[109]

specific surface area decreases local current density and adjusts electric field distribution, mitigating Mg electroplating.

Developing suitable cathode materials that facilitate efficient Mg-ion storage and cycling stability remains a challenge. Mu et al.^[110] presents a novel cathode material that integrates sulfur (S) functionality into two-dimensional 2D-MOFs, significantly enhancing Mg^{2+} storage capacity and cyclability. The introduction of S atoms altered the structural properties of the MOF, reducing the long-range order in the ab plane while increasing the out-of-plane order. This modification led to an increased interlayer distance, which contributed to enhanced Mg^{2+} storage performance. Cu-S5HHTP exhibited superior electrochemical properties compared to its nonsulfurized counterpart, Cu-HHTP, achieving a stable capacity of $\approx 500 \text{ mAh g}^{-1}$ after 15 cycles. Interestingly, the presence of S atoms mediated the interaction of Mg^{2+} with the $[\text{CuO}_4]$ node, effectively increasing the number of available Mg binding sites. This enhancement contributed to the superior capacity and stability observed in Cu-S5HHTP. Furthermore, S exhibited reversible redox behavior, which minimized the degradation of the MOF basal plane, maintaining the integrity of the material during cycling. MOF-derived carbon materials by selenization are used also as Mg ion cathodes. Liu et al.^[111] developed a novel heterojunction $\text{Ti}_3\text{C}_2/\text{CoSe}_2$ derived from MXene/ZIF-67, where CoSe_2 nanoparticles prevent the aggregation of MXene nanosheets, offering abundant active sites and excellent Mg storage capacity. Consequently, the $\text{Ti}_3\text{C}_2/\text{CoSe}_2$ cathode exhibited an exceptional rate capability of 75.7 mAh g^{-1} at 1000 mA g^{-1} and an impressive cycling life of over 500 cycles. Additionally, Wang et al.^[112] synthesized a composite of in situ carbon-coated cuprous sulfide ($\text{Cu}_2\text{S}@C$) using a sulfurization method derived from a Cu-MOF. This composite, evaluated as a cathode in a hybrid Mg^{2+}/Li^+ battery, delivered a discharge capacity of 400 mAh g^{-1} and retained $\approx 150 \text{ mAh g}^{-1}$ after 50 cycles in the nucleophilic hybrid electrolyte. To address the significant polarization and slow kinetics during the Mg insertion/deinsertion process, Cai et al.^[113] employed TiO_2 ultrafine nanocrystals derived from Ti-MOF as RMBs cathodes, achieving an ultralong battery life with a capacity retention of 75% after 1000 cycles. Xu et al.^[114] prepared CoSe porous polyhedra induced by Te heteroatoms with ZIF-67 as a template, enhancing ion transport and reducing reaction barriers, thus offering improved electrochemical performance.

4.3. Approach 3. Hybrid Approaches

By incorporating ILs into MOFs, the advantages and synergistic effects of both systems can be used, such as nonflammability and improved interfacial contact with electrodes. The ionic conductivity of these hybrid systems is determined by the quantity of IL and typically ranges from 10^{-6} to $10^{-3} \text{ S cm}^{-1}$.^[115] For instance, when $[\text{EMIM}_{0.8}\text{Li}_{0.2}][\text{TFSI}]$ IL is used in conjunction with MOF-525(Cu) to obtain Li-IL@MOF, the resulting hybrid material exhibits an ionic conductivity of $3 \times 10^{-4} \text{ S cm}^{-1}$ at RT and a higher Li^+ transference number (0.36 vs 0.14) than the original Li-IL.^[116] A similar system was used by Yang et al.^[117] for the development of quasi-solid-state sodium batteries. A sodium sulfonic ($-\text{SO}_3\text{Na}$)

group grafted to the UIO-based MOF ligand enhances Na^+ -ion conductivity. When combined with a sodium-based ionic liquid (Na-IL), specifically sodium bis(trifluoromethylsulfonyl)imide (NaTFSI) in 1-n-butyl-1-methylpyrrolidinium bis(trifluoromethylsulfonyl)imide (Bmpyr-TFSI), the Na-IL-laden sulfonated UIO-66 quasi-solid electrolyte achieves a Na^+ -ion conductivity of $3.6 \times 10^{-4} \text{ S cm}^{-1}$ at ambient temperature. This electrolyte has been integrated into quasi-solid-state sodium batteries, featuring a layered $\text{Na}_3\text{Ni}_{1.5}\text{TeO}_6$ cathode and a sodium-metal anode. The resultant quasi-solid-state $\text{Na}|\text{Na-IL}|UIOS\text{Na}|\text{Na}_3\text{Ni}_{1.5}\text{TeO}_6$ cells exhibit exceptional cycling performance, showcasing their potential for advanced energy storage applications.

Taking this approach into Mg batteries, Wei et al.^[118] incorporated $\text{Mg}(\text{TFSI})_2$ dissolved in $[\text{EMIM}][\text{TFSI}]$ to be used as quasi-solid state electrolyte. An ionic conductivity of $2.4 \times 10^{-4} \text{ S cm}^{-1}$ at 60°C was obtained. More importantly, it was concluded that the oxygen and fluorine-rich organic/inorganic composite interphase forming on the surface of the Mg anode was the origin of the Mg redox overpotential observed during battery operation. In further studies,^[119] it was demonstrated the importance remove all the guest solvent used to solvate Mg salts into the MOF structure otherwise the remaining DMF molecules will induce Mg passivation. Furthermore, magnesium deposition/dissolution reactions vary depending on the MOF structure, the guest anion species as well as the nature of the guest solvents. Figure 8a depicts the effect of the amount of DMF into the $\alpha\text{-Mg}_3[\text{HCOO}]_6$ MOF structure in the overpotential measurements using a Mg symmetric cell. In a recent work, Elnagar et al.^[120] examined the effect of chloride ions on Mg deposition/dissolution on Cu electrodes using a semi-solid electrolyte with 15–20% solvent content, comprising MOFs like $\alpha\text{-Mg}(\text{bp}3\text{dc})$ and $\alpha\text{-Mg}_3(\text{HCOO})_6$ with MgCl_2 and $\text{Mg}[\text{TFSI}]_2$. Chloride ions play a vital role in enhancing Mg dissolution. Increasing the potential limit to $4.0 \text{ V vs. Mg/Mg}^{2+}$ intensifies Mg dissolution and triggers Cu surface dissolution, creating new Mg deposition sites. Morphological analysis reveals pitting corrosion. Galvanostatic measurements show Cu oxidation and reduction, forming triangular nanoparticles. Electrochemical impedance spectroscopy analysis provides insights into structural changes during cycling, demonstrating the stability and potential of MOF-based semi-solid electrolytes for Mg-ion batteries. Bearing this in mind, the synthesis of 1D-hydrolyzed cellulose acetate (HCA) fiber along with a 3D MOF structure (e.g., ZIF-67, ZIF-4, and ZIF-8) and the combination with APC/LiCl electrolyte to form a gel polymer electrolyte was successfully developed by Wang et al.^[121]

Bearing this in mind, the synthesis of 1D-hydrolyzed cellulose acetate (HCA) fiber along with a 3D MOF structure (e.g., ZIF-67, ZIF-4, and ZIF-8) and the combination with APC/LiCl electrolyte to form a gel polymer electrolyte was successfully developed by Wang et al.^[121] Achieving ZIF-67@HCA a Mg-ion conductivity (4.42 mS cm^{-1}), a wide electrochemical window (3.93 V) and a capacity decay of 4% after 600 cycles at 30°C when it was used as a polymer electrolyte in a MoS_8/Mg battery configuration (Figure 8b-d). It has been demonstrated then that, co-intercalation approaches can be used as an alternative counter measure to combat the sluggishness of Mg^{2+} . The strategy involves pairing Mg^{2+} with Li^+ or Na^+ in dual-salt electrolytes to exploit the faster

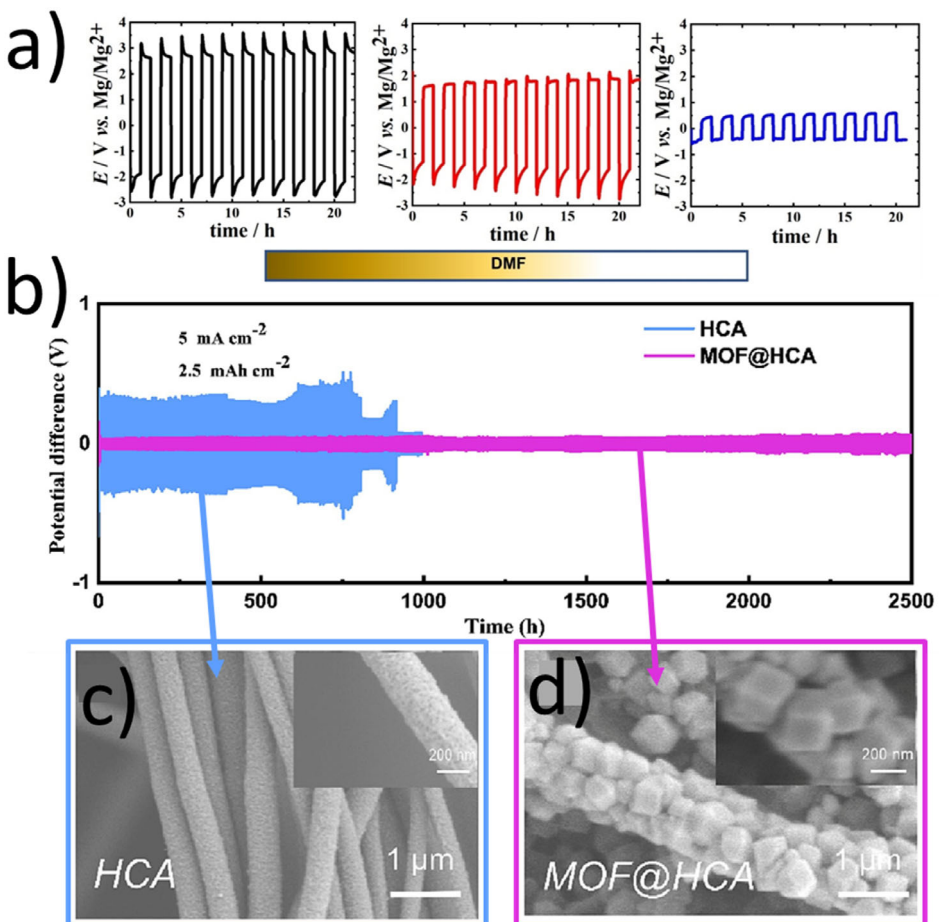


Figure 8. a) The galvanostatic measurement of Mg/Mg cell obtained depending on the amount of DMF molecules inside the MOF (from left: after synthesis and glyme solvent was added to solvate Mg²⁺ to right: all DMF molecules were removed from the structure. Reprinted with permission.^[119] b) Cycling curves of the Mg/Mg batteries at the current density of 5 mA cm⁻². c) SEM images of HCA film and d) MOF@HCA film. Reprinted with permission.^[121]

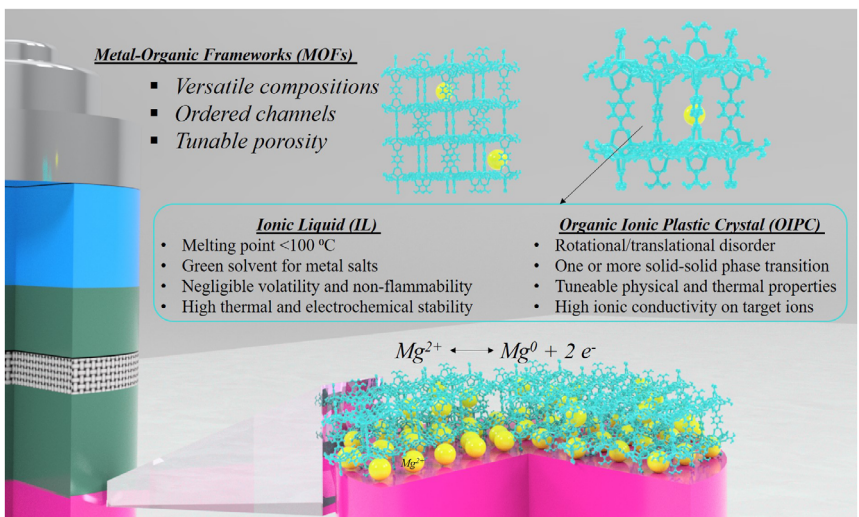
mobility of the latter with the aim to reach better electrochemical performance. Compared to pure magnesium electrodes, the SEI layer on Mg-Li alloys typically shows enhanced stability and ionic conductivity. A robust SEI layer can effectively mitigate the side reactions and preserve surface smoothness throughout cycling.

5. Final Remarks and Further Directions

This article provides a comprehensive review of the application progress of MOFs in RMBs. MOFs, with their adjustable porous structure, high specific surface area, and molecular-level designability, have shown great potential in various components of RMBs. Magnesium batteries have the potential to be a game-changer in the energy storage industry due to their high energy density, faster charging times, and increased safety. Although there are several challenges that need to be addressed, recent advancements in materials science and battery research have provided promising avenues for the development of practical magnesium batteries. As the demand for more efficient and sustainable energy storage solutions increases, the development of magnesium batteries could provide a viable alternative to traditional LIBs. The discovery of Grignard reagents was a key milestone

to realize reversible Mg deposition/stripping. However, only a few representative liquid electrolyte solutions have been developed with good voltage stability, high coulombic efficiency, and excellent compatibility with cathode/anode materials. In particular, the development of Mg solid electrolytes is the focus of future Mg electrolyte research, due to their merits of high safety and thermal stability.

As happened with LIBs, the understanding of the SEI formation and evolution is crucial for an efficient energy storage device. With a few nanometers thickness, comprises both organic and inorganic decomposition products from the electrolyte. An ideal artificial SEI should be thin ($\leq 2 \mu\text{m}$), possess high ionic conductivity, be dense and homogeneous, exhibit high mechanical strength, and effectively prevent nonuniform corrosion and deposition on the Mg metal anode. Future research should also prioritize developing scalable manufacturing technologies for artificial SEI films for Mg. Organic SEI layers may offer a unique self-healing capability but suffer from limited ion conductivity. Conversely, the low flexibility of inorganic SEI layers may restrict their broader application. A hybrid organic/inorganic SEI layer could provide a promising solution, combining the electronic insulation properties of inorganic components with the flexibility of organic materials, thereby enhancing performance.



Scheme 2. Characteristic of nanostructured interface approach to control SEI formation.

To achieve this, an engineering interface approach would not only improve the cycling performance but also the controlled nanoscale structure will provide information about the morphology of the SEI and volume expansion. A wide variety of artificial SEI films, including alloy-type, metal/halide-based, MOF-based, organic, inorganic, and hybrid layers, have been extensively developed for coin cells. Alloy-type and metal/halide-based SEIs may promote the outer deposition of Mg on the SEI due to their high electronic conductivity. MOF-based SEIs can be engineered to exhibit selective sieving actions for solvents or ion complexes by tuning pore size, ligands, and metal elements. The ordered pores of MOF-based materials may contribute to the rapid diffusion of magnesium ions and improve the charging and discharging rates and specific capacity of batteries. The technology of RMBs is relatively new, and the research and application of MOF-based electrodes for RMBs are still very limited. Further research and development by researchers are needed. For instance, future researchers can advance the field by focusing on the following areas: 1) Material design: Ongoing research should aim to design new Mg-based MOF materials that enhance electrochemical stability and conductivity, especially in applications involving high current densities and extended cycle life. 2) Structural optimization: By optimizing the porous structures and surface functionalization of MOFs, researchers can further improve stability within electrolytes and enhance ion migration efficiency. 3) Composite strategies: Developing innovative MOF-based composite materials that combine the strengths of various materials can lead to superior electrochemical performance. 4) Multiscale simulation: Utilizing computational chemistry and material simulation techniques can help predict and optimize the performance of MOF materials in RMBs applications. 5) Long-term stability: Examining the structural evolution and performance degradation mechanisms of MOF materials during prolonged cycling can lead to more durable battery systems. 6) Cost efficiency and scalability: Prioritizing the use of affordable raw materials and cost-effective synthesis methods can significantly boost the commercial feasibility of solid electrolytes derived from MOFs.

Besides, incorporating organic ionic plastic crystals (OIPCs) into solid electrolytes can enhance battery performance due to their crystalline lattice with local disorder. OIPCs exhibit high ionic conductivity, thermal stability, and mechanical flexibility, making them suitable for batteries, solar cells, and electrochromic devices.^[122] New OIPCs with pyrrolidinium, imidazolium, and phosphonium cations are promising for quasi-solid electrolytes. Anions such as BF₄⁻, PF₆⁻, and others have been explored.^[123] Wang et al.^[124] improved ion transport in solid-state LIBs using Li⁺ doped [C₂mpyr][FSI] in a PVDF matrix, achieving high specific capacity and stability. Additionally, impressive ionic conductivity was obtained by confining PBu₄TFSI in a covalent-organic framework.^[125] Further advancements could be made by incorporating [N₁₁₁₁][Mg(μ-η¹-η¹-TFSAs)₃] and [N₁₁₂₂][Mg(μ-η¹-η¹-TFSAs)(η²-TFSAs)₂] into MOF structures.

Specifically, a key issue is the understanding of the phenomenon of charge transport at metal/electrolyte interfaces and within the novel electrolyte materials. This will provide a basis for understanding the behavior of such materials, and thus moving toward overcoming the performance limitations. In the future, it is expected that the implementation of MOF/OIPC material (**Scheme 2**) as cornerstone to obtain efficient solid electrolytes by elucidating the correlation between chemical structures and physicochemical. As well as better electrode interfaces are suggested as a promising approach to pave the way to magnesium-based batteries.

Acknowledgements

M.S. acknowledges the funding from the European Union H2020 Program under the Marie Skłodowska Curie global fellowship (ROCHE, 101026163). This study forms part of the Advanced Materials program and was supported by MCIN with funding from European Union NextGenerationEU (PRTR-C17.I1) and by the Basque Government under the IKUR program.

Conflict of Interest

The authors declare no conflict of interest.

Keywords: magnesium batteries · metal–organic frameworks · organic ionic plastic crystals · polymers · solid-state electrolytes

- [1] L. Montanarella, P. Panagos, *Land Use Policy* **2021**, *100*, 104950.
- [2] A. Sikora, *ERA Forum* **2021**, *21*, 681.
- [3] J. Zhu, W. Xu, M. Knapp, M. S. Dewi Darma, L. Mereacre, P. Su, W. Hua, X. Liu-Théato, H. Dai, X. Wei, H. Ehrenberg, *Cell Rep. Phys. Sci.* **2023**, *4*, 101464.
- [4] T. Or, S. W. D. Gourley, K. Kaliyappan, A. Yu, Z. Chen, *Carbon Energy* **2020**, *2*, 6.
- [5] Y. Lu, J. Chen, *Nat. Rev. Chem.* **2020**, *4*, 127.
- [6] L. da Silva Lima, M. Quartier, A. Buchmayr, D. Sanjuan-Delmás, H. Laget, D. Corbisier, J. Mertens, J. Dewulf, *Sustainable Energy Technol. Assess.* **2021**, *46*, 101286.
- [7] A. Manthiram, X. Yu, S. Wang, *Nat. Rev. Mater.* **2017**, *2*, 16103.
- [8] P. Jaumaux, Q. Liu, D. Zhou, X. Xu, T. Wang, Y. Wang, F. Kang, B. Li, G. Wang, *Angew. Chem., Int. Ed.* **2020**, *59*, 9134.
- [9] C. Mendes-Felipe, J. C. Barbosa, S. Gonçalves, N. Pereira, C. M. Costa, J. L. Vilas-Vilela, S. Lanceros-Mendez, *Compos. Sci. Technol.* **2020**, *199*, 108363.
- [10] M. Guo, C. Yuan, T. Zhang, X. Yu, *Small* **2022**, *18*, 2106981.
- [11] F. Duffner, N. Kronemeyer, J. Tübke, J. Leker, M. Winter, R. Schmuck, *Nat. Energy* **2021**, *6*, 123.
- [12] D. Monti, A. Ponrouch, R. B. Araujo, F. Barde, P. Johansson, M. R. Palacín, *Front. Chem.* **2019**, *7*, 79.
- [13] Y. Liang, H. Dong, D. Aurbach, Y. Yao, *Nat. Energy* **2020**, *5*, 646.
- [14] F. Bella, S. De Luca, L. Fagioli, D. Versaci, J. Amici, C. Francia, S. Bodoardo, *Nanomaterials* **2021**, *11*, 810.
- [15] C. Wei, L. Tan, Y. Zhang, Z. Wang, J. Feng, Y. Qian, *Energy Storage Mater.* **2022**, *52*, 299.
- [16] S. Chen, S. Fan, H. Li, Y. Shi, H. Y. Yang, *Coord. Chem. Rev.* **2022**, *466*, 214597.
- [17] I. D. Johnson, B. J. Ingram, J. Cabana, *ACS Energy Lett.* **2021**, *6*, 1892.
- [18] D. Wu, J. Zeng, H. Hua, J. Wu, Y. Yang, J. Zhao, *Nano Res.* **2020**, *13*, 335.
- [19] J. J. Pryke, R. M. Kennard, S. A. Cussen, *Energy Rep.* **2022**, *8*, 83.
- [20] E. Lancry, E. Levi, Y. Gofer, M. Levi, G. Salitra, D. Aurbach, *Chem. Mater.* **2004**, *16*, 2832.
- [21] D. Muthuraj, S. Mitra, *Mater. Res. Bull.* **2018**, *101*, 167.
- [22] C. Li, W. Wu, Y. Liu, X. Yang, Z. Qin, Z. Jia, X. Sun, *J. Power Sources* **2022**, *520*, 230853.
- [23] J. H. Yang, E. G. Ahn, J. H. Lee, *J. Power Sources* **2022**, *520*, 230828.
- [24] N. Tran, N. Do Van Thanh, M. L. P. Le, *Chem. - Eur. J.* **2021**, *27*, 9198.
- [25] F. Peng, Y. Chu, Y. Li, Q. Pan, G. Yang, L. Zhang, S. Hu, F. Zheng, H. Wang, Q. Li, *J. Energy Chem.* **2022**, *71*, 434.
- [26] X.-F. Ma, H.-Y. Li, W. Ren, D. Gao, F. Chen, J. Diao, B. Xie, G. Huang, J. Wang, F. Pan, *J. Mater. Sci. Technol.* **2023**, *153*, 56.
- [27] P. Shan, Y. Gu, L. Yang, T. Liu, J. Zheng, F. Pan, *Inorg. Chem.* **2017**, *56*, 13411.
- [28] X. Xue, X. Song, A. Tao, W. Yan, X. L. Zhang, Z. Tie, Z. Jin, *Nano Res.* **2023**, *16*, 2399.
- [29] W. Miao, H. Peng, S. Cui, J. Zeng, G. Ma, L. Zhu, Z. Lei, Y. Xu, *iScience* **2024**, *27*, 109811.
- [30] X. Sun, P. Bonnick, V. Duffort, M. Liu, Z. Rong, K. A. Persson, G. Ceder, L. F. Nazar, *Energy Environ. Sci.* **2016**, *9*, 2273.
- [31] S. Dey, J. Lee, S. Britto, J. M. Stratford, E. N. Keyzer, M. T. Dunstan, G. Cibin, S. J. Cassidy, M. Elgaml, C. P. Grey, *J. Am. Chem. Soc.* **2020**, *142*, 19588.
- [32] J. Zhang, J. Liu, M. Wang, Z. Zhang, Z. Zhou, X. Chen, A. Du, S. Dong, Z. Li, G. Li, G. Cui, *Energy Environ. Sci.* **2023**, *16*, 1111.
- [33] F. Liu, T. Wang, X. Liu, L. Z. Fan, *Adv. Energy Mater.* **2021**, *11*, 2000787.
- [34] S. R. Mousavi, H. Hosseini, *J. Mater. Sci.: Mater. Electron.* **2023**, *34*, 818.
- [35] X. Liu, A. Du, Z. Guo, C. Wang, X. Zhou, J. Zhao, F. Sun, S. Dong, G. Cui, *Adv. Mater.* **2022**, *34*, 2201886.
- [36] Z. Song, Z. Zhang, A. Du, S. Dong, G. Li, G. Cui, *Adv. Mater.* **2021**, *33*, 2100224.
- [37] J. Bae, H. Park, X. Guo, X. Zhang, J. H. Warner, G. Yu, *Energy Environ. Sci.* **2021**, *14*, 4391.
- [38] M. Mao, X. Fan, W. Xie, H. Wang, L. Suo, C. Wang, *Adv. Sci.* **2023**, *10*, 2207563.
- [39] R. Shah, V. Mittal, E. Matsil, A. Rosenkranz, *Adv. Mech. Eng.* **2021**, *13*.
- [40] H. Liu, S. Tan, Z. Wang, Y. Chen, J. Yue, D. Wang, G. Huang, J. Wang, F. Pan, *ChemSusChem* **2024**, *17*, e202301589.
- [41] X. Zheng, Y. Yuan, D. Gu, D. Li, L. Zhang, L. Wu, J. Wang, M. Fichtner, F. Pan, *Nano Lett.* **2024**, *24*, 10734.
- [42] P. De, M. Pumera, *Small* **2024**, *20*, 2404227.
- [43] H. Weiqin, 3D Printed Magnesium Battery, <https://www.think3d.in/3d-printed-high-capacity-magnesium-batteries-developed-by-taiwan-researchers/> (accessed: June 2016).
- [44] Z. Zhao, B. Nian, Y. Lei, L. Zhao, M. N. Hedhili, D. Guo, Z. Shi, W. Zhao, J. K. El-Demellawi, Y. Wang, Y. Zhu, K. Xu, H. N. Alshareef, *Adv. Mater.* **2024**, *36*, 2402626.
- [45] C. Liebenow, *J. Appl. Electrochem.* **1997**, *27*, 221.
- [46] D. Aurbach, Z. Lu, A. Schechter, Y. Gofer, H. Gizbar, R. Turgeman, Y. Cohen, M. Moshkovich, E. Levi, *Nature* **2000**, *407*, 13.
- [47] Y. Viestfrid, M. D. Levi, Y. Gofer, D. Aurbach, *J. Electroanal. Chem.* **2005**, *576*, 183.
- [48] M. S. Ding, T. Diemant, R. J. Behm, S. Passerini, G. A. Giffin, *J. Electrochem. Soc.* **2018**, *165*, A1983.
- [49] K. Sato, G. Mori, T. Kiyosu, T. Yaji, K. Nakanishi, *Sci. Rep.* **2020**, *10*, 7362.
- [50] R. Horia, D. T. Nguyen, A. Y. S. Eng, Z. W. Seh, *Batteries Supercaps* **2022**, *5*, e202200011.
- [51] C. Liao, N. Sa, B. Key, A. K. Burrell, L. Cheng, L. A. Curtiss, J. T. Vaughney, J.-J. Woo, L. Hu, B. Pan, Z. Zhang, *J. Mater. Chem. A* **2015**, *3*, 6082.
- [52] S. Hebie, H. Phuong, K. Ngo, J. Lepre, C. Ilojoi, L. Cointeaux, R. Berthelot, F. Alloin, *ACS Appl. Mater. Interfaces* **2017**, *9*, 28377.
- [53] L. Xue, D. D. DesMarteau, W. T. Pennington, *Solid State Sci.* **2005**, *7*, 311.
- [54] W. Ren, D. Wu, Y. NuLi, D. Zhang, Y. Yang, Y. Wang, J. Yang, *ACS Energy Lett.* **2021**, *6*, 3212.
- [55] W. Ren, M. Cheng, Y. Wang, D. Zhang, Y. Yang, J. Yang, J. Wang, Y. NuLi, *Batteries Supercaps* **2022**, *5*, e202200263.
- [56] B. Dlugatch, M. Mohankumar, R. Attias, B. M. Krishna, Y. Elias, Y. Gofer, D. Zitoun, D. Aurbach, *ACS Appl. Mater. Interfaces* **2021**, *13*, 54894.
- [57] T. Mandai, H. Naya, H. Masu, *J. Phys. Chem. C* **2023**, *127*, 7987.
- [58] R. Jay, A. W. Tomich, J. Zhang, Y. Zhao, A. De Gorostiza, V. Lavallo, J. Guo, *ACS Appl. Mater. Interfaces* **2019**, *11*, 11414.
- [59] S.-B. Son, T. Gao, S. P. Harvey, K. X. Steirer, A. Stokes, A. Norman, C. Wang, A. Cresce, K. Xu, C. Ban, *Nat. Chem.* **2018**, *10*, 532.
- [60] Y. NuLi, J. Yang, R. Wu, *Electrochem. Commun.* **2005**, *7*, 1105.
- [61] N. Amir, Y. Vestfrid, O. Chusid, Y. Gofer, D. Aurbach, *J. Power Sources* **2007**, *174*, 1234.
- [62] Z. Zhao-Karger, J. E. Mueller, X. Zhao, O. Fuhr, T. Jacob, M. Fichtner, *RSC Adv.* **2014**, *4*, 26924.
- [63] F. Bertasi, F. Sepehr, G. Pagot, S. J. Paddison, V. Di Noto, *Adv. Funct. Mater.* **2016**, *26*, 4859.
- [64] F. Bertasi, C. Hettige, F. Sepehr, X. Bogle, G. Pagot, K. Vezzù, E. Negro, S. J. Paddison, S. G. Greenbaum, M. Vittadello, V. Di Noto, *ChemSusChem* **2015**, *8*, 3069.
- [65] T. Watkins, A. Kumar, D. A. Buttry, *J. Am. Chem. Soc.* **2016**, *138*, 641.
- [66] M. Kar, Z. Ma, L. M. Azofra, K. Chen, M. Forsyth, D. R. MacFarlane, *Chem. Commun.* **2016**, *52*, 4033.
- [67] M. Kar, O. Tutusaus, D. R. MacFarlane, R. Mohtadi, *Energy Environ. Sci.* **2019**, *12*, 566.
- [68] Z. Zhao-Karger, X. Zhao, D. Wang, T. Diemant, R. J. Behm, M. Fichtner, *Adv. Energy Mater.* **2015**, *5*, 1401155.
- [69] T. Kakibe, J. Hishii, N. Yoshimoto, M. Egashira, M. Morita, *J. Power Sources* **2012**, *203*, 195.
- [70] G. T. Cheek, W. E. O'Grady, S. Z. El Abedin, E. M. Moustafa, F. Endres, *J. Electrochem. Soc.* **2008**, *155*, D91.
- [71] T. D. Gregory, R. J. Hoffman, R. C. Winterton, *J. Electrochem. Soc.* **1990**, *137*, 775.
- [72] Q. Wang, H. Li, R. Zhang, Z. Liu, H. Deng, W. Cen, Y. Yan, Y. Chen, *Energy Storage Mater.* **2022**, *51*, 630.
- [73] L. N. Skov, J. B. Grinderslev, A. Rosenkranz, Y. S. Lee, T. R. Jensen, *Batteries Supercaps* **2022**, *5*, e202200163.
- [74] Y. Zhan, W. Zhang, B. Lei, H. Liu, W. Li, *Front. Chem.* **2020**, *8*, 125.
- [75] N. M. Vignesh, S. S. Jayabalakrishnan, S. Selvasekarapandian, P. Kavitha, S. A. Hazaana, R. M. Naachiyan, *Ionics* **2024**, *30*, 1469.
- [76] F. Chen, J. Yu, R. Li, F. Shi, X. Che, K. C. Chan, Y. Sun, W. Xue, Z.-L. Xu, *J. Power Sources* **2024**, *611*, 234780.
- [77] M. Armand, *Solid State Ionics* **1983**, *9–10*, 745.
- [78] A. Patrick, M. Glasse, R. Latham, R. Linford, *Solid State Ionics* **1986**, *18–19*, 1063.
- [79] K. Chen, D. F. Shriver, *Chem. Mater.* **1991**, *3*, 771.
- [80] C. Liebenow, *Electrochim. Acta* **1998**, *43*, 1253.

- [81] K. Nivetha, K. Vijaya Kumar, N. Krishna Jyothi, K. V. Kamma, *J. Mater. Sci.: Mater. Electron.* **2024**, *35*, 277.
- [82] Y. Shao, N. N. Rajput, J. Hu, M. Hu, T. Liu, Z. Wei, M. Gu, X. Deng, S. Xu, K. S. Han, J. Wang, Z. Nie, G. Li, K. R. Zavadil, J. Xiao, C. Wang, W. A. Henderson, J.-G. Zhang, Y. Wang, K. T. Mueller, K. Persson, J. Liu, *Nano Energy* **2015**, *12*, 750.
- [83] M. Salado, R. Fernández de Luís, T. H. Smith, M. Hasanpoor, S. Lanceros-Mendez, M. Forsyth, *Batteries Supercaps* **2024**, *7*, e202400134.
- [84] S. Chen, M. Zhou, D. Zhang, S. Zhang, Y. Zhao, M. Pan, Y. Wang, Y. Sun, J. Yang, J. Wang, Y. NuLi, *Adv. Funct. Mater.* **2024**, *34*, 2408535.
- [85] H. Park, H.-K. Lim, S. H. Oh, J. Park, H.-D. Lim, K. Kang, *ACS Energy Lett.* **2020**, *5*, 3733.
- [86] T. Wen, B. Qu, S. Tan, G. Huang, J. Song, Z. Wang, J. Wang, A. Tang, F. Pan, *Energy Storage Mater.* **2023**, *55*, 816.
- [87] B. Yang, L. Xia, R. Li, G. Huang, S. Tan, Z. Wang, B. Qu, J. Wang, F. Pan, *J. Mater. Sci. Technol.* **2023**, *157*, 154.
- [88] Y. Sun, M. Pan, Y. Wang, A. Hu, Q. Zhou, D. Zhang, S. Zhang, Y. Zhao, Y. Wang, S. Chen, M. Zhou, Y. Chen, J. Yang, J. Wang, Y. NuLi, *Angew. Chem., Int. Ed.* **2024**, *63*, e202406585.
- [89] Y. Zhang, J. Li, W. Zhao, H. Dou, X. Zhao, Y. Liu, B. Zhang, X. Yang, *Adv. Mater.* **2022**, 34.
- [90] U. Pal, D. Rakov, B. Lu, B. Sayahpour, F. Chen, B. Roy, D. R. MacFarlane, M. Armand, P. C. Howlett, Y. S. Meng, M. Forsyth, *Energy Environ. Sci.* **2022**, *15*, 1907.
- [91] Y. Li, J. G. Shapter, H. Cheng, G. Xu, G. Gao, *Particuology* **2021**, *58*, 1.
- [92] M. Salado, E. Lizundia, *Mater. Today Energy* **2022**, *28*, 101064.
- [93] A. K. Thakur, M. Majumder, S. P. Patole, K. Zaghib, M. V. Reddy, *Mater. Adv.* **2021**, *2*, 2457.
- [94] B. Zhu, Z. Liang, D. Xia, R. Zou, *Energy Storage Mater.* **2019**, *23*, 757.
- [95] J. S. Park, J. H. Kim, S. J. Yang, *Bull. Korean Chem. Soc.* **2021**, *42*, 148.
- [96] Z. Wang, R. Tan, H. Wang, L. Yang, J. Hu, H. Chen, F. Pan, *Adv. Mater.* **2018**, *30*, 1704436.
- [97] M. L. Aubrey, R. Ameloot, B. M. Wiers, J. R. Long, *Energy Environ. Sci.* **2014**, *7*, 667.
- [98] Y. Zheng, J. Guo, D. Ning, Y. Huang, W. Lei, J. Li, J. Li, G. Schuck, J. Shen, Y. Guo, Q. Zhang, H. Tian, H. lan, H. Shao, *J. Mater. Sci. Technol.* **2023**, *144*, 15.
- [99] S. S. Park, Y. Tulchinsky, M. Dincă, *J. Am. Chem. Soc.* **2017**, *139*, 13260.
- [100] E. M. Miner, S. S. Park, M. Dincă, *J. Am. Chem. Soc.* **2019**, *141*, 4422.
- [101] Y. Yoshida, T. Yamada, Y. Jing, T. Toyao, K. I. Shimizu, M. Sadakiyo, *J. Am. Chem. Soc.* **2022**, *144*, 8669.
- [102] H. K. Hassan, A. Farkas, A. Varzi, T. Jacob, *Batteries Supercaps* **2022**, *5*, e202200260.
- [103] W. Zhou, Y. Li, S. Xin, J. B. Goodenough, *ACS Cent. Sci.* **2017**, *3*, 52.
- [104] J. Luo, Y. Li, H. Zhang, A. Wang, W. S. Lo, Q. Dong, N. Wong, C. Povinelli, Y. Shao, S. Chereddy, S. Wunder, U. Mohanty, C. K. Tsung, D. Wang, *Angew. Chem., Int. Ed.* **2019**, *58*, 15313.
- [105] C. Glaser, Z. Wei, S. Indris, P. Klement, S. Chatterjee, H. Ehrenberg, Z. Zhao-Karger, M. Rohnke, J. Janek, *Adv. Energy Mater.* **2023**, *13*, 2301980.
- [106] C. T. Lee, M. W. Shin, *Surf. Interfaces* **2021**, *22*, 100845.
- [107] W. Zhang, R. Taheri-Ledari, M. Saeidirad, F. S. Qazi, A. Kashtiaray, F. Ganjali, Y. Tian, A. Maleki, *J. Environ. Chem. Eng.* **2022**, *10*, 108836.
- [108] C. Hu, C. Wang, Y. Xia, F. Xu, T. Li, *Mater. Lett.* **2023**, *341*, 134241.
- [109] Y. Wang, F. Cheng, Y. Huang, C. Cai, Y. Fu, *Energy Storage Mater.* **2023**, *61*, 102911.
- [110] Y. Mu, J. Nyakuchena, Y. Wang, J. R. Wilkes, T. Luo, M. Goldstein, B. Elander, U. Mohanty, J. L. Bao, J. Huang, D. Wang, *Angew. Chem., Int. Ed. Engl.* **2024**, *63*, e202409286.
- [111] F. Liu, T. Wang, X. Liu, N. Jiang, L.-Z. Fan, *Chem. Eng. J.* **2021**, *426*, 130747.
- [112] W. Wang, Y. Yang, Y. NuLi, J. Zhou, J. Yang, J. Wang, *J. Power Sources* **2020**, *445*, 227325.
- [113] X. Cai, Y. Xu, Q. An, Y. Jiang, Z. Liu, F. Xiong, W. Zou, G. Zhang, Y. Dai, R. Yu, L. Mai, *Chem. Eng. J.* **2021**, *418*, 128491.
- [114] R. Xu, H. Xiao, Y. Chen, X. Gao, Z. Zhang, H. Sun, X. Chen, C. Peng, L. Cui, *Mater. Today Phys.* **2024**, *42*, 101361.
- [115] X. Yu, N. S. Grundish, J. B. Goodenough, A. Manthiram, *ACS Appl. Mater. Interfaces* **2021**, *13*, 24662.
- [116] M. F. Majid, H. F. M. Zaid, C. F. Kait, A. Ahmad, K. Jumbri, *Nanomaterials* **2022**, *12*, 1076.
- [117] P. Yang, J. Qiang, J. Chen, Z. Zhang, M. Xu, L. Fei, *Angew. Chem., Int. Ed.* **2025**, *64*, e202414770.
- [118] Z. Wei, R. Maile, L. M. Rieger, M. Rohnke, K. Müller-Buschbaum, J. Janek, *Batteries Supercaps* **2022**, *5*, e202200318.
- [119] H. K. Hassan, P. Hoffmann, T. Jacob, *ChemSusChem* **2024**, *17*, e202301362.
- [120] M. M. Elnagar, H. K. Hassan, L. A. Kibler, T. Jacob, *Batteries Supercaps* **2025**, *8*, e202400420.
- [121] Y. Wang, Y. Huang, Y. Fu, *Carbohydr. Polym.* **2023**, *314*, 120919.
- [122] D. R. MacFarlane, M. Forsyth, P. C. Howlett, M. Kar, S. Passerini, J. M. Pringle, H. Ohno, M. Watanabe, F. Yan, W. Zheng, S. Zhang, J. Zhang, *Nat. Rev. Mater.* **2016**, *1*, 15005.
- [123] F. Nti, G. W. Greene, H. Zhu, P. C. Howlett, M. Forsyth, X. Wang, *Mater. Adv.* **2021**, *2*, 1683.
- [124] X. Wang, H. Zhu, G. W. Greene, Y. Zhou, M. Yoshizawa-Fujita, Y. Miyachi, M. Armand, M. Forsyth, J. M. Pringle, P. C. Howlett, *Adv. Mater. Technol.* **2017**, *2*, 1700046.
- [125] J. Wang, L. Liu, Y. Liu, X. M. Zhang, J. Li, *Small* **2023**, *19*, 2207831.
- [126] Z. Ma, D. R. MacFarlane, M. Kar, *Batteries Supercaps* **2019**, *2*, 115.
- [127] Z. Zhang, Z. Cui, L. Qiao, J. Guan, H. Xu, X. Wang, P. Hu, H. Du, S. Li, X. Zhou, S. Dong, Z. Liu, G. Cui, L. Chen, *Adv. Energy Mater.* **2017**, *7*, 1602055.
- [128] Y. Yu, W. Wang, Z. Jing, X. Zheng, X. Geng, J. Li, *J. Alloys Compd.* **2016**, *688*, 605.
- [129] L. Kong, Q. Zhang, *J. Energy Chem.* **2019**, *33*, 167.
- [130] J. Xie, J. Wang, H. R. Lee, K. Yan, Y. Li, F. Shi, W. Huang, A. Pei, G. Chen, R. Subbaraman, J. Christensen, Y. Cui, *Sci. Adv.* **2025**, *4*, eaat5168.
- [131] S. Li, Y. Huang, W. Ren, C. Luo, L. Zhao, J. Liu, X. Li, M. Wang, H. Cao, *Chem. Eng. J.* **2021**, *420*, 130002.
- [132] J. Park, J. Jeong, Y. Lee, M. Oh, M.-H. Ryou, Y. M. Lee, *Adv. Mater. Interfaces* **2016**, *3*, 1600140.
- [133] T. Wen, S. Tan, R. Li, X. Huang, H. Xiao, X. Teng, H. Jia, F. Xiong, G. Huang, B. Qu, J. Song, J. Wang, A. Tang, F. Pan, *ACS Nano* **2024**, *18*, 11740.
- [134] C. Li, A. Shyamsunder, B. Key, Z. Yu, L. F. Nazar, *Joule* **2023**, *7*, 2798.
- [135] Y. Du, Y. Chen, S. Tan, J. Chen, X. Huang, L. Cui, J. Long, Z. Wang, X. Yao, B. Shang, G. Huang, X. Zhou, L. Li, J. Wang, F. Pan, *Energy Storage Mater.* **2023**, *62*, 102939.
- [136] H. Yang, Z. Chang, Y. Qiao, H. Deng, X. Mu, P. He, H. Zhou, *Angew. Chem., Int. Ed.* **2020**, *59*, 9377.
- [137] L. Fan, Z. Guo, Y. Zhang, X. Wu, C. Zhao, X. Sun, G. Yang, Y. Feng, N. Zhang, *J. Mater. Chem. A* **2020**, *8*, 251.
- [138] M. Liu, L. Yang, H. Liu, A. Amine, Q. Zhao, Y. Song, J. Yang, K. Wang, F. Pan, *ACS Appl. Mater. Interfaces* **2019**, *11*, 32046.
- [139] L. Cao, D. Li, T. Deng, Q. Li, C. Wang, *Angew. Chem., Int. Ed.* **2020**, *59*, 19292.
- [140] Y. Xu, L. Gao, L. Shen, Q. Liu, Y. Zhu, Q. Liu, L. Li, X. Kong, Y. Lu, H. Bin Wu, *Matter* **2020**, *3*, 1685.
- [141] Z.-J. Zheng, Q. Su, Q. Zhang, X.-C. Hu, Y.-X. Yin, R. Wen, H. Ye, Z.-B. Wang, Y.-G. Guo, *Nano Energy* **2019**, *64*, 103910.
- [142] Y. Zhang, J. Li, W. Zhao, H. Dou, X. Zhao, Y. Liu, B. Zhang, X. Yang, *Adv. Mater.* **2022**, *34*, 2108114.

Manuscript received: February 26, 2025

Version of record online: March 25, 2025